Thermodynamics of the two-dimensional Heisenberg classical honeycomb lattice

Jacques Curély*
Centre de Physique Moléculaire Optique et Hertzienne, Université Bordeaux I, 351 Cours de la Libération, 33405 Talence Cédex, France

Francesc Lloret and Miguel Julve
Departament de Química Inorgànica, Facultat de Química de la Universitat de València, Dr Moliner 50, 46100 Burjassot (València), Spain

(Received 27 March 1998)

In this article we adapt a previous work concerning the two-dimensional (2D) Heisenberg classical square lattice [Physica B **245**, 263 (1998)] to the case of a honeycomb lattice. Closed-form expressions of the main thermodynamic functions of interest are derived in the zero-field limit. Notably, near absolute zero (i.e., the critical temperature), we derive the values of the critical exponents $\alpha=0$, $\eta=-1$, $\gamma=3$, and $\nu=1$, as for the square lattice, thus proving their universal character. A very simple model allows one to give a good description of the low-temperature behaviors of the product χT. For a 2D-compensated antiferromagnet, we derive simple relations between the characteristics of the maximum of the susceptibility curve $T(\chi_{\max})$ and $\chi_{\max}$ and the involved exchange energies. Therefore, owing to the knowledge of $T(\chi_{\max})$ and $\chi_{\max}$, one can directly obtain the respective values of these energies. Finally, we show that the theoretical model allows one to fit correctly experimental susceptibility data of the recently synthetized compound $Mn_2(bpm)(ox)_2\cdot 6H_2O$ characterized by a 2D classical honeycomb lattice (where ''bpm'' and ''ox'' are the abbreviations for the ligands bipyrimidine and oxalate, respectively). [S0163-1829(98)04434-8]

I. INTRODUCTION

For three decades low-dimensional (low-*d*) physics has known important advances and, more particularly, the subbranch of low-*d* magnetism.[1] The reasons for such a strong interest have multiple origins. In a first step, a lot of theoretical works have been published for interpreting the static and dynamic properties of one-dimensional (1D) and two-dimensional (2D) magnetic materials and, more generally, the critical phenomena appearing in such systems. The maximum effort was attained in the 1970s, but this level has remained about constant since then, notably due to the recent progresses in molecular chemistry with respect to the synthesis of new 1D and 2D compounds. In a second step, from the middle of the 1980s, the discovery of layered copper oxide compounds showing a high-T_c superconductivity as well as a 2D antiferromagnetic behavior has still accentuated the initial interest.[2]

The prototype of 2D lattices is the well-known K_2NiF_4 compound.[3] Let us recall that its structure can be considered as being derived from the cubic (perovskite) $KNiF_3$ structure by the addition of an extra layer of KF between the NiF_2 sheets so that, by this simple fact, a 3D antiferromagnetic lattice is transformed into a magnetic layer structure characterized by a square unit cell. Of course, a lot of compounds showing a different unit cell structure have been synthetized and studied.[1] In particular, among these specimens, $MnTiO_3$ has been early investigated.[4] This compound is characterized by an ilmenite structure in which the Mn^{2+} and Ti^{4+} ions occupy alternated hexagonal layers and Mn^{2+} layers are separated from each other by two oxygene and one Ti^{4+} sheets. From a magnetic point of view, it has been shown that the Mn^{2+} spins are directed antiparallel (in the ground state) within each layer perpendicular to the hexagonal *c* axis.[5] Magnetic susceptibility measured by Akimitsu *et al.*[6] on a single crystal as well as that on a powder sample by Stickler *et al.*[7] shows no anomaly at the Néel temperature T_N determined from neutron diffraction measurement[6] and a 2D Heisenberg antiferromagnetic behavior above T_N. Unfortunately, more recently, Yamauchi *et al.*[8] have pointed out that this behavior is strongly perturbated by the presence of magnetic dipole interactions between the Mn^{2+} ions, thus leading in fact to a global magnetic anisotropy. The aim of the present article is to examine a new class of 2D honeycomb lattices in which organic ligands are inserted between the magnetic ions so that, by distancing them, it allows to confer a highly 2D magnetic behavior.

In recent works it has been shown how the polymerization through bis-chelating ligands such as 2,2′-bipyrimidine (bpm) and oxalate (ox) using suitable precursors as building blocks provides a new strategy to design novel honeycomb-layered materials.[9,10] For example compounds of formula $[M_2(bpm)(ox)_2]\cdot nH_2O$, with $M=$Mn(II) ($n=6$) and Cu(II) ($n=5$) exhibiting local spins of associated quantum numbers 5/2 and 1/2, respectively, show magnetic isolated sheetlike structures (the shortest interlayer metal-metal separation being larger than 6.5 Å) in which the spin carriers are bridged by bis-chelating bpm and ox groups forming ring-shaped hexamers (Fig. 1). Given that both bpm and ox have a remarkable efficiency to mediate a relatively strong antiferromagnetic coupling between metal ions separated by more than 5 Å,[10–14] alternating antiferromagnetic interactions are expected to occur in these compounds. In addition, due to the presence of the magnetic ions Mn(II) and Cu(II), one may expect that the magnetic behaviors of these alternating magnetic planes will be correctly described by that of an alter-

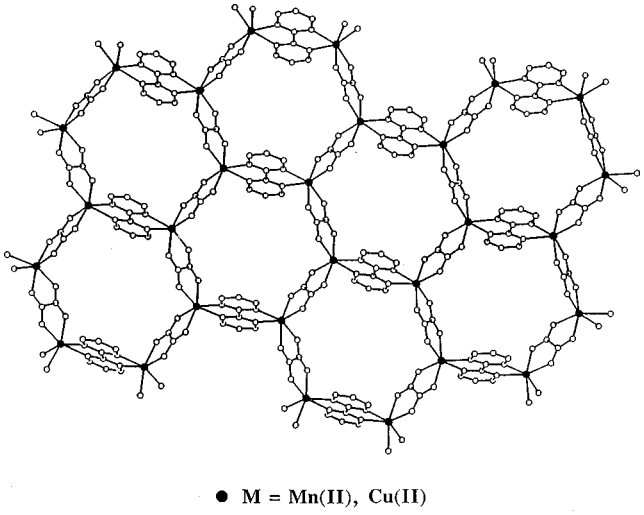

FIG. 1. Crystal structure of complex $M_2(\mathrm{bpm})(\mathrm{ox})_2\cdot 6H_2O$: view of a sheet perpendicular to the *xy* plane (hydrogen atoms and water molecules have been omitted for clarity).

nating magnetic honeycomb-layered lattice through a 2D Heisenberg model. More particularly, if the lattice is composed of ions Mn(II), the associated spin moments can be assimilated to classical ones and the formalism used very recently for a classical square lattice can be employed through an adequate adaptation.[15,16]

In the first version of this theoretical work,[15] each host site among the $(2N+1)^2$ sites (i,j) of the square lattice carries a classical spin moment and the isotropic exchange couplings between nearest neighbors are characterized by the associated exchange energies J_1 and J_2 for the horizontal and vertical lines, respectively. More recently, a complete study has detailed the case of finite or infinite Heisenberg classical square lattices characterized by two types of exchange energies per line and row.[16] In a first part,[16(a)] the closed-form expression of the zero-field partition function in the thermodynamic limit has been rigorously established. Moreover, it has been shown that absolute zero plays the important role of critical temperature so that the critical domain is quasi-infinite. In other words, for nonzero temperatures, there is no long-range order and the quantum fluctuations play a major role, thus favoring the short-range order; at $T=0$ K, rigorously, a stable long-range order appears due to the fact that quantum fluctuations become negligible. In a second part,[16(b)] the specific heat, the spin-spin correlations, the static susceptibility as well as the correlation length for an infinite lattice have been derived. Notably, owing to the low-temperature study of their respective closed-form expressions, it has allowed one to calculate the value of the critical exponents, i.e., $\alpha=0$, $\eta=-1$, $\gamma=3$, and $\nu=1$. In the present article, by transforming the square unit cell into a hexagonal one, we are going to show that it is possible to adapt the previous theoretical results to the case of a honeycomb lattice; in particular, that will permit one to derive the same analytical values for α, η, γ, and ν, thus confirming their universal character whatever the unit cell structure. More particularly, we shall recall that the result $\nu=1$ allows one to underline the major role played by the quantum fluctuations in the critical domain.

Thus, in the present work, we shall mainly focus on the behavior of the static susceptibility χ for three fundamental reasons. (i) The low-temperature study of χ gives a good idea of the mechanisms which are involved in the construction of the 2D arrangement; notably, we shall show that a very simple model can allow one to describe the various behaviors of the product χT. (ii) For 2D-compensated antiferromagnets, we shall point out that, from the study of the characteristic maximum of the susceptibility curve, one can directly derive the respective values of the involved exchange energies. (iii) The possibility of interpreting experimental susceptibility data obtained on 2D Heisenberg classical honeycomb lattices recently synthetized[9,10] offers a very important opportunity for testing the validity of the theoretical model. In particular, we shall focus on the compound $Mn_2(\mathrm{bpm})(\mathrm{ox})_2\cdot 6H_2O$ where the involved quantum spins ($S=5/2$) are assimilated to classical ones. Therefore, under these conditions and owing to the preceding remarks concerning the deep nature of the involved exchange couplings in such materials, we shall show that it allows one to fit correctly the experimental susceptibility curves in a wide range of temperature.

II. THEORETICAL MODEL

A. General considerations

The previous theoretical works concerning 2D Heisenberg classical square lattices[15,16] can be easily extended to the case where each horizontal line (respectively, vertical row) is described by a sequence of alternating exchange energies J_0 and J_0' (respectively, J and J_1), with one of the four energies J_0, J_0', J, or J_1 showing a vanishing value. Then, under these conditions, the lattice is composed of hexagonal unit cells [see Figs. 2(a) and 2(b)]. Therefore, if each moment is submitted to an external magnetic field **B** applied along the *z* axis of quantization, the corresponding Hamiltonian may be written in the most general case:

$$H=\sum_{i=-N}^{N-1}\sum_{j=-N}^{N-1}H_{i,j}^{\mathrm{ex}}+\sum_{i=-N}^{N}\sum_{j=-N}^{N}H_{i,j}^{\mathrm{mag}}, \tag{1}$$

with

$$H_{i,j}^{\mathrm{ex}}=[J_0'\mathbf{S}_{i,j-1}+J_0\mathbf{S}_{i,j+1}+J\mathbf{S}_{i+1,j}+J_1\mathbf{S}_{i-1,j}]\cdot\mathbf{S}_{i,j},$$

$$H_{i,j}^{\mathrm{mag}}=-G_{i,j}S_{i,j}^{z}B, \tag{2}$$

where

$$G_{i,j}=G \quad \text{if } i+j \text{ even}, \quad G_{i,j}=G' \quad \text{if } i+j \text{ odd}. \tag{3}$$

$S_{i,j}^{z}$ is the *z* component of the classical vector operator $\mathbf{S}_{i,j}$ associated with the site labeled (i,j) (the spin quantum number $S_{i,j}$ is large enough for $[S_{i,j}^{x},S_{i,j}^{y}]$ to be negligible compared to $S_{i,j}^{x}S_{i,j}^{y}$, the classical spin approximation). G and G' are the associated Landé factors and characterize the magnetic ions of the unit cell. In addition, in our writing, $J>0$ denotes an antiferromagnetic coupling.

The partition function $Z_N(B)$ of the spin lattice may be directly written as

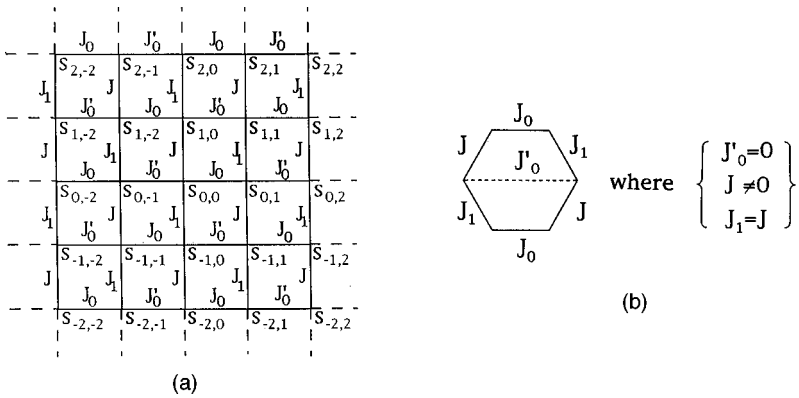

FIG. 2. (a) Structure of a 2D lattice composed of classical spins and characterized by a square unit cell and (b) transformation of the square unit cell into a hexagonal one (honeycomb lattice).

$$Z_N(B)=\int d\mathbf{S}_{-N,-N}\cdots\int d\mathbf{S}_{i,j}\cdots\int d\mathbf{S}_{N,N}\times\exp\left(-\beta\left[\sum_{i=-N}^{N-1}\sum_{j=-N}^{N-1}(H_{i,j}^{\mathrm{ex}}+H_{i,j}^{\mathrm{mag}})+H_{N,N}^{\mathrm{mag}}\right]\right),\tag{4}$$

where $\beta=1/k_BT$ is the Boltzmann factor (not to be confused with the critical exponent β_c). At this step it must be noticed that the calculation of the field-dependent partition function $Z_N(B)$ is plainly more complicated because of the presence of the further term $H_{i,j}^{\mathrm{mag}}$ in the exponential argument, for each site (i,j). This aspect will not be examined in the present article.

B. Evaluation of the zero-field partition function of an infinite honeycomb lattice

If we consider Eq. (4) in the zero-field limit, the Hamiltonian involved in the exponential argument is thus reduced to the exchange one $H_{i,j}^{\mathrm{ex}}$; because of the presence of classical spin moments, all the operators $H_{i,j}^{\mathrm{ex}}$ commute and we have

$$\exp\left(-\beta\sum_{i=-N}^{N-1}\sum_{j=-N}^{N-1}H_{i,j}^{\mathrm{ex}}\right)=\prod_{i=-N}^{N-1}\prod_{j=-N}^{N-1}\exp(-\beta H_{i,j}^{\mathrm{ex}}).\tag{5}$$

Moreover, the particular nature of $H_{i,j}^{\mathrm{ex}}$ allows one to separate the contributions corresponding to the exchange coupling involving classical spins belonging to a same line i of the layer (i.e., $\mathbf{S}_{i,j-1}$, $\mathbf{S}_{i,j+1}$, and $\mathbf{S}_{i,j}$) or to a same row j (i.e., $\mathbf{S}_{i-1,j}$, $\mathbf{S}_{i+1,j}$, and $\mathbf{S}_{i,j}$). In fact, for each of the four contributions (one per bond connected to spin $\mathbf{S}_{i,j}$), we have to expand a factor such as $\exp(-A\mathbf{S}_1\cdot\mathbf{S}_2)$ where A is $\beta J_0'$, βJ_0, βJ, or βJ_1 ($\mathbf{S}_1$ and $\mathbf{S}_2$ are considered as unit vectors). If we call $\Theta_{1,2}$ the angle between vectors $\mathbf{S}_1$ and $\mathbf{S}_2$, respectively, characterized by the couples of angular variables (θ_1,ϕ_1) and (θ_2,ϕ_2), it is possible to expand $\exp(-A\cos\Theta_{1,2})$ on the infinite basis of spherical harmonics:

$$\exp(-A\cos\Theta_{1,2})=4\pi\sum_{l=0}^{+\infty}\left(\frac{\pi}{2A}\right)^{1/2}I_{l+1/2}(-A)\times\sum_{m=-l}^{+l}Y_{l,m}^{*}(\mathbf{S}_1)Y_{l,m}(\mathbf{S}_2),\tag{6}$$

where the $I_{l+1/2}(-A)$'s are modified Bessel functions of the first kind and where $\mathbf{S}_1$ and $\mathbf{S}_2$ symbolically represent the couples (θ_1,ϕ_1) and (θ_2,ϕ_2). Let λ_l be the radial factor [note that if j is the corresponding exchange energy, $\lambda_l(-\beta j)$ is the modified Bessel function of the first kind, $I_{l+1/2}(-\beta j)$ multiplied by the factor $(\pi/2\beta j)^{1/2}$]. Subsequently, one can note that each local operator $\exp(-\beta H_{i,j}^{\mathrm{ex}})$ is finally expanded on a basis of eigenfunctions (the spherical harmonics), whereas the λ_l's are nothing more than the associated eigenvalues. Under these conditions and for the general lattice described by Fig. 2(a), the zero-field partition function $Z_N(0)$ directly appears as a characteristic polynomial and may be written as

$$Z_N(0)=(4\pi)^{4N(2N+1)}\sum_{l_{N,-N}}\lambda_{l_{N,-N}}(-\beta J_0)\sum_{l'_{N,-N}}\lambda_{l'_{N,-N}}(-\beta J)\times\cdots\times\sum_{l_{-N,N-1}}\lambda_{l_{-N,N-1}}(-\beta J_0')$$
$$\times\cdots\times\sum_{m_{N,-N}=-l_{N,-N}}^{+l_{N,-N}}\sum_{m'_{N,-N}=-l'_{N,-N}}^{+l'_{N,-N}}\times\cdots\times\sum_{m_{-N,N-1}=-l_{-N,N-1}}^{+l_{-N,N-1}}\prod_{k_1=-N}^{N}\prod_{k_2=-N}^{N}\int d\mathbf{S}_{k_1,k_2}Y_{l'_{k_1+1,k_2},m'_{k_1+1,k_2}}(\mathbf{S}_{k_1,k_2})$$
$$\times Y_{l_{k_1,k_2-1},m_{k_1,k_2-1}}(\mathbf{S}_{k_1,k_2})Y_{l_{k_1,k_2},m_{k_1,k_2}}^{*}(\mathbf{S}_{k_1,k_2})Y_{l'_{k_1,k_2},m'_{k_1,k_2}}^{*}(\mathbf{S}_{k_1,k_2}).\tag{7}$$

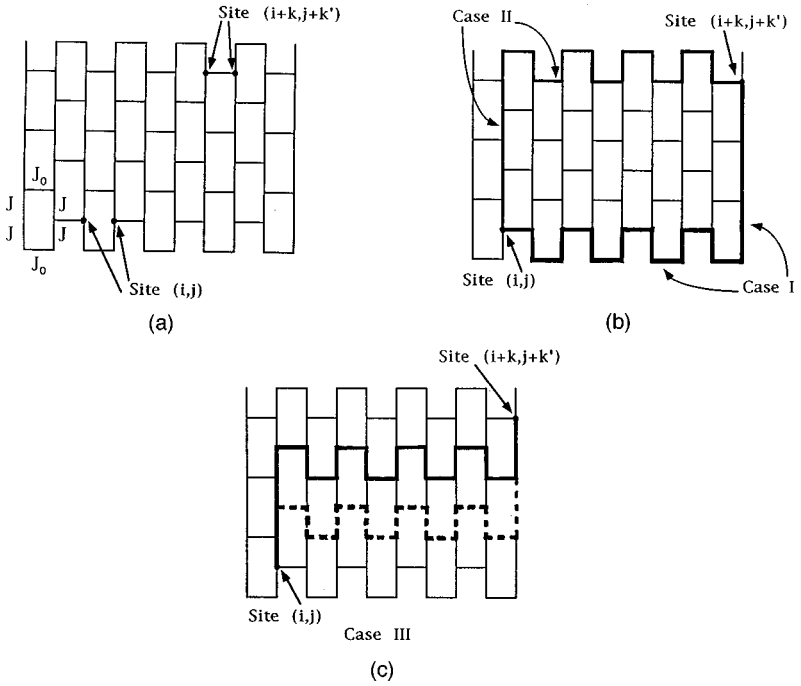

FIG. 3. (a) Description of the lattice sites and (b) and (c) examples of correlation paths for a honeycomb lattice composed of classical spins isotropically coupled.

Therefore, in a second step, a global work of integration must be achieved over all the angular variables characterizing all the states of the classical spins belonging to the whole lattice. Thus, by expanding all the l summations in Eq. (7), $Z_N(0)$ can be considered as a λ_l-polynomial expansion in which each term is composed of a product of radial factors λ_l and angular ones $F_{K,K'}$ characterizing each lattice site (K,K') where $F_{K,K'}$ is the current integral. Note that, in the formal writing of Eq. (7), the number of spherical harmonics represents the total number of bonds characterizing each site. In other words, for the honeycomb lattice, one or two spherical harmonics must be replaced by unity according to whether the corresponding site (K,K') has three or two bonds with its nearest neighbors (in-site or edge site). Consequently, from now, we take into account the hexagonal character of the unit cell by assuming $J_1=J$ and $J_0'=0$ [see Figs. 2(a) and 2(b)].

For expressing the beginning of the characteristic polynomial given by Eq. (7), we use a numerical argument which has been previously employed for the classical square lattice:[15,16(a)] For nonzero temperatures and for a same argument $\beta|j|$, the functions $\lambda_l(\beta|j|)$ defined above rapidly decrease when l increases. Consequently, this is the radial factor involving the product of functions λ_l which is preponderant and allows a classification of each term in the λ_l-polynomial expansion of $Z_N(0)$. The angular factor composed of a product of integrals $F_{K,K'}$ only intervenes in this expansion by the bias of a numerical coefficient which does not play a major role. Therefore, in this framework, when the total radial factor is known for each term of the characteristic polynomial, i.e., when the current integers $l_{K,K'}$ and $l'_{K,K'}$ have been chosen for the whole lattice, the global integration process concerning all the imbricated integrals $F_{K,K'}$ leads to the determination of integers $m_{K,K'}$ and $m'_{K,K'}$ which exclusively characterize the angular factor.

Due to the fact that the construction of the polynomial structure of $Z_N(0)$ is quite analogous to that one previously detailed for the 2D Heisenberg classical square lattice,[15,16(a)] we have recalled it in a separate appendix. More particularly, we briefly show that, for a finite honeycomb lattice, the zero-field partition function $Z_N(0)$ does not have a unique expression so that the analytical problem is unsolvable. However, from a physical point of view, the most interesting situation occurs when the lattice becomes infinite, i.e., in the thermodynamic limit. Therefore, using the numerical argument concerning the classification of the various eigenvalues λ_l, we have established the beginning of the polynomial expansion of $Z_N(0)$ [see Eq. (A3)]. At this step, due to the hexagonal structure of the unit cell, the work of integration over the angular variables differs and must be thoroughly detailed. Of course, it is plainly influenced by the new structure of the unit cell. Thus the lattice can be considered as the juxtaposition of rectangles linked horizontally with the nearest-neighbor rectangles by the middle of their vertical sides [see Fig. 3(a)]. Therefore, the horizontal edges as well as all the other horizontal in-lines are made of square zigzags, whereas the vertical ones are continuous lines. Under these conditions, the main difference with the square-lattice structure appears for the treatment of the horizontal lines, which can be then considered as the particular junction of two consecutive horizontal lines of the previous square lattice.

At the beginning of the integration work, one can start at the four infinite lattice edges simultaneously. Indeed, for these sites, the integers l and l' concerning the horizontal zigzag edges (respectively, l' for the vertical ones) can be chosen independently with respect to the l''s (respectively, l's) characterizing the in-bonds linked with the corresponding edge because they are exclusively shared between con-

secutive edge sites. Then, after having achieved this choice, the work of integration concerns the other infinite in-horizontal zigzags and in-vertical rows which are closer and closer to the lattice heart. In this respect one must note that each new horizontal zigzag or vertical row behaves itself like an edge. For illustrating this property let us consider the two types of sites appearing in the hexagonal structure. If the site (K,K') belonging to the horizontal zigzag K shows a left horizontal bond, the integers $l_{K,K'-1}$ and $l'_{K+1,K'}$ are shared by two consecutive sites belonging to the same zigzag and can be chosen independently from the third one $l'_{K,K'}$ which characterizes the vertical bond connected with the similar following horizontal zigzag $K-2$. If the site (K,K') shows a right horizontal bond, for example, the integer $l'_{K+1,K'}$ is already determined by the integration over the preceding horizontal zigzag $K+2$; the remaining integers $l_{K,K'}$ and $l'_{K,K'}$ are shared by two consecutive sites belonging to the same zigzag K and can be chosen independently from $l'_{K+1,K'}$ [see Fig. 3(a)]. Note that for the vertical rows each site is always characterized by two vertical bonds and a single horizontal one; in all cases, the integers $l'_{K+1,K'}$ and $l'_{K,K'}$ can be chosen independently from $l_{K,K'-1}$ (if the site shows a left horizontal bond) or $l_{K,K'}$ (if the site shows a right horizontal bond).

Consequently, using the preceding remark concerning the numerical property of functions λ_l and $\lambda_{l'}$, the contribution to the higher-degree term of the λ_l-polynomial expansion of $Z_N(0)$ is obtained when all the integers l and l' are equal to a common positive (or null) value; notably, its upper value is derived for $l=l'=0$ $(m=m'=0)$. For the highest value of the second-rank term, one also considers that all the in-bonds are characterized by vanishing coefficients $l_{\rm in}$ and $l'_{\rm in}$ (and subsequently $m_{\rm in}$ and $m'_{\rm in}$). In that case, among all the edge integrals those containing three spherical harmonics are reduced to a product of two spherical ones due to the fact that the spherical harmonics characterizing the corresponding in-bond reduces to unity [see Fig. 3(a)]. Thus we derive that, inside each edge, after integrating over the angular variables involved in each current integral $F_{K,K'}$, the edge integers l and l' (respectively, m and m') are equal to a common value. Moreover, due to the fact that, at the four lattice corners, the current integral only contains two spherical harmonics characterizing two consecutive edges, we globally show that all the edge coefficients l and l' (respectively, m and m') are equal to a common positive value $l_{\rm ed}$ (respectively, $m_{\rm ed}$). Consequently, in the thermodynamic limit, $Z_N(0)$ may be written as

$$Z_N(0)\sim(4\pi)^{3N(2N+1)}\left[\left\{\frac{\Lambda_0}{(4\pi)^3}\right\}^{N(2N+1)}+\sum_{l=2}^{+\infty}(\Lambda_l)^{N(2N+1)}\sum_{\{m=-l\}}^{\{m=+l\}}\prod_{k_1=-N}^{+N}\prod_{k_2=-N}^{+N}F_{k_1,k_2}(m)\right.$$
$$\left.+\left\{\frac{\Lambda_0^{\rm in}}{(4\pi)^3}\right\}^{N(2N-3)}\sum_{l_{\rm ed}=1}^{+\infty}(2l_{\rm ed}+1)\left\{\frac{\Lambda_{l_{\rm ed}}^{\rm ed}}{(4\pi)^3}\right\}^{4N}+\cdots\right]\quad\text{as}\quad N\to+\infty, \tag{8}$$

where $1/4\pi$ and $F(m)$ are the current values of integral $F_{K,K'}$ [for $m=0$ and for each current value of m belonging to the set $\{m\}$ in the leader term; note that this symbolical notation concerns the $3N(2N+1)-2$ summations over coefficients $m_{i,j}$ and $m'_{i,j}$]. The factor $2l_{\rm ed}+1$, which appears in the second-rank term, is due to the summation over $m_{\rm ed}$ achieved for each edge site and characterizes the degeneracy of the corresponding eigenvalue $\lambda_{l_{\rm ed}}$. The factors Λ_0, Λ_l, $\Lambda_0^{\rm in}$, and $\Lambda_{l_{\rm ed}}^{\rm ed}$ represent the product $\lambda_l(-\beta J_0)\lambda_l(-\beta J)^2$, with $l=0$ for Λ_0 and $\Lambda_0^{\rm in}$, $l\geqslant 2$ (and even) for Λ_l, $l_{\rm ed}\geqslant 1$ for $\Lambda_{l_{\rm ed}}^{\rm ed}$. As for the terms represented by the ellipsis they are constituted by a product of functions $\lambda_l(-\beta j)$ (with $j=J_0$ or J) in which most of these functions describing the in-bonds are characterized by different coefficients $l\geqslant 1$. In addition, one must note that these terms do not have a unique analytical expression (because of the undetermination of coefficients m and m' which characterize the final angular factor; see the Appendix).

If one factorizes the term Λ_0 in Eq. (8), ratios appear, such as Λ_l/Λ_0 and $\Lambda_{l_{\rm ed}}^{\rm ed}/\Lambda_0$ [in fact, ratios such as $\lambda_l(\beta|j|)/\lambda_0(\beta|j|)$], which are always lower than unity (in absolute value) due to the fact that, for the same argument $\beta|j|$, the function $\lambda_l(\beta|j|)$ rapidly decreases when l increases. When N tends to infinity, i.e., in the thermodynamic limit, the quantities $(\Lambda_l/\Lambda_0)^{N(2N+1)}$ and $(\Lambda_{l_{\rm ed}}^{\rm ed}/\Lambda_0)^{4N}$ rapidly vanish so that the second part of the higher-degree term and the upper limit of the second-rank term in Eq. (8) become negligible with respect to unity as well as the nonanalytical terms represented by the ellipsis, which are of lower rank. Therefore, $Z_N(0)$ finally has an analytical expression and may be written

$$Z_N(0)\sim[\lambda_0(-\beta J_0)\lambda_0(-\beta J)^2]^{N(2N+1)}\quad\text{as}\quad N\to+\infty. \tag{9}$$

One can note that this result appears to be independent of the choice of edge coefficients l and l' used at the beginning of the integration process, thus confirming the fact that edge effects are negligible in the thermodynamic limit.[16(a)] Finally, it has been shown[16(a)] that, even at $T=0$ K, the preceding reasoning prevails: For infinite arguments all the λ_l functions have the same asymptotic behavior whatever $l\geqslant 1$, i.e., $\exp(\beta|j|)/\beta|j|$, so that all the terms of the character-

istic polynomial given by Eq. (7) become equivalent to the corresponding higher-degree term obtained for vanishing l's and l''s, i.e., $[\lambda_0(-\beta J_0)\lambda_0(-\beta J)^2]^{N(2N+1)}$. In other words, when the square unit cell is transformed into a hexagonal one, at 0 K, $Z_N(0)$ is directly proportional to $[\lambda_0(-\beta J_0)\lambda_0(-\beta J)^2]^{N(2N+1)}$. Of course, this particular aspect also prevails for all the thermodynamic functions derived from $Z_N(0)$. Indeed, these functions are characterized by a fraction the denominator of which is precisely $Z_N(0)$ and the numerator a derivative of $Z_N(0)$ with respect to the parameter $\beta=1/k_BT$ (specific heat) or to the external applied field B, expressed in the vanishing-B limit (spin-spin correlation, susceptibility). Therefore, they are independent of the factor of proportionality appearing in $Z_N(0)$. Thus this very particular case will not be considered in the present article because its mathematical treatment is similar to that used for nonvanishing temperatures, in the thermodynamic limit.

Finally, one must notice that the result given by Eq. (9) is very close to that obtained by Fisher[17] for an open classical spin chain. By assuming $J_0=0$, one finds again Fisher's result, whereas if $J=0$, one retrieves the zero-field partition function of $N(2N+1)$ dimers, as expected. Moreover, as for the 2D Heisenberg classical square lattice,[16(a)] $Z_N(0)$ appears as the product of the zero-field partition functions, respectively, associated with the horizontal lines (dimers) and the vertical rows (spin chains) which compose the lattice (theorem 1). Note that $Z_N(0)$ can be also seen as the product of the zero-field partition functions of horizontal square zigzag chains and vertical dimers, respectively. *This result has been previously justified[16(a)] by the fact that we mainly deal with classical moments isotropically coupled, which constitutes a generalization of the corresponding theorem 1 obtained for a square unit cell.*[16(a)]

C. Evaluation of the specific heat of an infinite honeycomb lattice

At this step one can note that, owing to the exact knowledge of the zero-field partition function $Z_N(0)$ in the thermodynamic limit and the correlative definition of the specific heat C_N,

$$C_N=k_B\beta^2\,\frac{\partial^2\,\ln Z_N(0)}{\partial\beta^2}, \tag{10}$$

one can directly derive the specific heat per site (i,j), C, in terms of hyperbolic functions:

$$C=k_B\left[\frac{3}{2}-\frac{1}{2}\left(\frac{\beta J_0}{\sinh(-\beta J_0)}\right)^2-\left(\frac{\beta J}{\sinh(-\beta J)}\right)^2\right] \quad \text{as } N\to+\infty. \tag{11}$$

The study of this quantity will not be detailed in the present article, but in the next subsection, Sec. III A, we shall determine the associated critical exponent α in the general discussion concerning the low-temperature behaviors, i.e., near the critical point.

D. Evaluation of the spin-spin correlation for an infinite honeycomb lattice

Due to the isotropic aspect of couplings, the three spin-spin correlations $\langle S^x_{i,j}S^x_{i+k,j+k'}\rangle$, $\langle S^y_{i,j}S^y_{i+k,j+k'}\rangle$, and $\langle S^z_{i,j}S^z_{i+k,j+k'}\rangle$ are equal; for simplifying the various calculations, we are exclusively going to focus on the Z-Z spin-spin correlation, which may be defined as

$$\begin{aligned}\langle S^z_{i,j}S^z_{i+k,j+k'}\rangle=\frac{(4\pi)^{3N(2N+1)}}{Z_N(0)}&\sum_{l_{N,-N}}\lambda_{l_{N,-N}}(-\beta J_0)\sum_{l'_{N,-N}}\lambda_{l'_{N,-N}}(-\beta J)\times\cdots\times\sum_{l_{-N,N-1}}\lambda_{l_{-N,N-1}}(-\beta J'_0)\\ &\times\cdots\times\sum_{m_{N,-N}=-l_{N,-N}}^{+l_{N,-N}}\sum_{m'_{N,-N}=-l'_{N,-N}}^{+l'_{N,-N}}\times\cdots\times\sum_{m_{-N,N-1}=-l_{-N,N-1}}^{+l_{-N,N-1}}\prod_{k_1=-N}^{N}\prod_{k_2=-N}^{N}\\ &\times\int d\mathbf{S}_{k_1,k_2}X_{k_1,k_2}Y_{l'_{k_1+1,k_2},m'_{k_1+1,k_2}}(\mathbf{S}_{k_1,k_2})Y_{l_{k_1,k_2-1},m_{k_1,k_2-1}}(\mathbf{S}_{k_1,k_2})Y^*_{l_{k_1,k_2},m_{k_1,k_2}}(\mathbf{S}_{k_1,k_2})Y^*_{l'_{k_1,k_2},m'_{k_1,k_2}}(\mathbf{S}_{k_1,k_2}),\end{aligned} \tag{12}$$

with

$$\begin{aligned}X_{k_1,k_2}&=\cos\,\theta_{k_1,k_2}\quad[(k_1,k_2)=(i,j),\quad(k_1,k_2)=(i+k,j+k')],\\ &=1\quad[(k_1,k_2)\neq(i,j),\quad(k_1,k_2)\neq(i+k,j+k')],\end{aligned} \tag{13}$$

and where $Z_N(0)$ is the zero-field partition function given by Eq. (9). As for the formal integral expression of $Z_N(0)$ [cf. Eq. (7)], note that, in the analogous writing of the spin-spin correlation, the spherical harmonics characterizing the nonexisting bonds must be replaced by unity.

In a preceding article[16(b)] we have detailed the calculus of the spin-spin correlations for a 2D Heisenberg classical square lattice. Notably, due to the great similarity between the respective polynomial expressions of $Z_N(0)$ and $\langle S^z_{i,j} S^z_{i+k,j+k'} \rangle$ [here given by Eqs. (7) and (13)], we have derived that the λ_l-polynomial expansion of the Z-Z spin-spin correlation can be evaluated owing to the same method which has led to the closed-form expression of the zero-field partition function $Z_N(0)$, in the thermodynamic limit. However, we have noted that, because of the presence of extra terms $\cos \theta_{K,K'}$ at sites $(K,K')=(i,j)$ and $(i+k,j+k')$, it is necessary to distinguish the sites belonging to the ''correlation rectangle'' constructed between sites (i,j), $(i,j+k')$, $(i+k,j+k')$, and $(i+k,j)$ and those belonging to the remaining part of lattice called the ''wing domain.'' Therefore, the results derived for a square unit cell can be easily transposed to the case of the hexagonal one.

1. Wing contribution to the spin-spin correlation for an infinite honeycomb lattice

For all the sites belonging to the wing domain and as for $Z_N(0)$, the work of integration begins at the infinite lattice edges. At this step it is necessary to choose integers l and l' for the edge bonds, independently of the current ones l_{in} and l'_{in} characterizing the in-bonds. After that, one may consider the other infinite in-horizontal zigzags and in-vertical rows in the direction of the correlation rectangle. Due to the preceding work of integration, they behave themselves as edge zigzags or vertical lines as has been explained above during the calculation of $Z_N(0)$. In the thermodynamic limit, the upper ''wing contribution'' to the λ_l-polynomial expansion appearing in the numerator of the Z-Z spin-spin correlation is also obtained when all the coefficients l_{in} are equal to a common value $l_{\text{in}}=0$. Consequently, the edge integrals reduce to the product of two spherical harmonics and it allows one to derive that all the current edge coefficients l_{ed} are equal to a common positive (or null) value. In this respect, one must be precise about an important point which is a direct consequence of the imbricated character of integrals $F_{K,K'}$ describing all the spin statements: All the bonds belonging to the wing domain and connected with the edges of the correlation rectangle are characterized by vanishing coefficients l_{in} and l'_{in}. This result is obtained without achieving the integration work over all the infinite zigzags and rows which cross themselves inside the correlation rectangle. As for the upper value of the second-rank term, there is a slight difference with respect to the corresponding one obtained for $Z_N(0)$ and characterized by all the l's and the l''s equal to a common value $l>0$. As seen in the Appendix, the current integral $F_{K,K'}$ does not vanish if l is even. But at sites (i,j) and $(i+k,j+k')$, $F_{K,K'}$ contains the extra term $\cos \theta_{K,K'}$ and vanishes if all the l's are even. In other words, the only nonvanishing contribution of the second-rank terms is characterized by a mixture of coefficients l and l' showing different values and has no analytical contribution, as the corresponding one of the polynomial expansion of $Z_N(0)$ (see Appendix). However, in the thermodynamic limit, these terms become negligible with respect to the higher-degree one.

Therefore, several conclusions may be derived: *(i) In the thermodynamic limit, only the higher-degree term of the polynomial expansion of the Z-Z spin-spin correlation numerator (characterized by vanishing coefficients l and l′) is selected so that* $\langle S^z_{i,j} S^z_{i+k,j+k'} \rangle$ *appears to be independent of the choice of edge coefficients* l_{ed}*, as expected; (ii) the correlations between sites (i,j) and* $(i+k,j+k')$ *are exclusively achieved owing to paths constructed by means of bonds belonging to the correlation rectangle and independently of the rectangle size* (theorem 2 or the confinement theorem).

2. Contribution of the ''correlation'' domain to the spin-spin correlation for an infinite honeycomb lattice

As expected, the heart of the reasoning (concerning the in-sites belonging to the correlation rectangle) mainly depends on the lattice unit cell structure. At this step one can recall that, as the wing domain, the correlation rectangle is composed of horizontal square zigzags and vertical continuous rows. Subsequently, it becomes necessary to detail the specific work of integration for a honeycomb lattice, inside the correlation rectangle. In the most general case [see Fig. 3(a)], at site $(i+k,j+k')$ [respectively, at site (i,j)], there are three bonds and the corresponding integral $F_{K,K'}$—which contains the extra term $\cos \theta_{K,K'}$, i.e., $2(\pi/3)^{1/2} Y_{1,0}(\mathbf{S}_{K,K'})$—is composed of four spherical harmonics. However, if one uses the decomposition law of the product $\cos \theta_{K,K'} Y_{L_{K,K'},M_{K,K'}}(\mathbf{S}_{K,K'})$ versus $Y_{L_{K,K'}+1,M_{K,K'}}(\mathbf{S}_{K,K'})$ and $Y_{L_{K,K'}-1,M_{K,K'}}(\mathbf{S}_{K,K'})$, where $Y_{L_{K,K'},M_{K,K'}}(\mathbf{S}_{K,K'})$ is one of the three spherical harmonics involved in $F_{K,K'}$, $F_{K,K'}$ is finally made of two terms, each of them showing a product of three spherical harmonics. However, due to the ''wing'' contribution (evaluated in the thermodynamic limit) which imposes a vanishing coefficient l or l' for the bonds linked with the edges of the correlation rectangle, $F_{K,K'}$ reduces to two spherical harmonics. In fact and as expected, the choice of the remaining coefficients l and l' is mainly conditioned by the position of site $(i+k,j+k')$ [respectively, site (i,j)] in the hexagonal unit cell considered as a rectangular one [see Fig. 3(a)]. For simplifying the discussion let us consider site $(i+k,j+k')$. If this site is characterized by a vanishing left bond $(J'_0=0)$, one has automatically $l_{i+k,j+k'-1}=0$ and $l_{i+k,j+k'}=0$ due to the infinite wing contribution so that one has to determine $l'_{i+k+1,j+k'}$ and $l'_{i+k,j+k'}$. As for the square unit cell, there are two possible choices: $l'_{i+k+1,j+k'}=1$, $l'_{i+k,j+k'}=0$ or $l'_{i+k+1,j+k'}=0$, $l'_{i+k,j+k'}=1$, due to the cumulative product of functions $\lambda_l(-\beta J_0)$ and $\lambda_{l'}(-\beta J)$ characterizing the infinite horizontal zigzag $i+k$. If there is a left bond $(J_0 \neq 0)$, one has $l_{i+k,j+k'}=0$ (no right bond) and $l'_{i+k+1,j+k'}=0$ due to the infinite wing contribution. That time one has to determine $l_{i+k,j+k'-1}$ and $l'_{i+k,j+k'}$; for the same reasons just evoked above, there are two possible choices $l_{i+k,j+k'-1}=1$, $l'_{i+k,j+k'}=0$ or $l_{i+k,j+k'-1}=0$,

$l'_{i+k,j+k'}=1$. In other words, there are two possible beginnings for the correlation paths, as for the infinite square lattice;[15,16(b)] consequently, it becomes necessary to detail the general process of integration.

At this step one must notice that, due to the lattice symmetries and as observed for $Z_N(0)$, the work of integration inside the correlation rectangle can be achieved according to two equivalent processes, i.e., starting from site $(i+k,j+k')$ for going to site (i,j) (and reciprocally) or starting simultaneously from sites (i,j) and $(i+k,j+k')$ in the direction of the lattice heart. Before beginning this work let us recall an important point. In the wing domain, it has been observed that, due to the work of integration on the preceding horizontal zigzags and vertical rows, each new zigzag or row behaves itself like an edge. This aspect also prevails for the zigzags and rows crossing inside the correlation rectangle and not yet taken into account by the integration work inside the wing domain.

For simplifying the discussion without losing its general character, let us suppose that integration starts at site $(i+k,j+k')$, with $i\geqslant 0$, $j\geqslant 0$, $k>0$, and $k'>0$; note that, from now, the position of site $(i+k,j+k')$ characterized by the presence or the absence of a left bond has no importance in the following reasoning. As shown for the square lattice,[16(b)] there are two possibilities: (i) The vertical row $j+k'$ is fixed, and integration concerns infinite horizontal zigzags between sites $(i+k,j+k')$ and (i,j). *At this step one can notice that one must consider horizontal zigzags, the structure of which is imposed by that one of the starting edge containing site* $(i+k,j+k')$, *due to the fact that one must respect the hexagonal unit cell structure*. (ii) The horizontal zigzag $i+k$ is fixed, and integration concerns infinite vertical rows K' such as $j\leqslant K'\leqslant j+k'$. Of course, we are going to show that both methods lead to the same result.

In a first step let us consider that row $j+k'$ is fixed. Each new infinite horizontal zigzag K showing the same geometrical structure as that of the starting edge $i+k$ behaves like an edge; the cumulative product of eigenvalues $\lambda_l(-\beta J_0)$ and $\lambda_{l'}(-\beta J)$ imposes vanishing coefficients l and l' characterizing all the bonds of zigzag K, except for the coefficients $l'_{K,j+k'}$, which are equal to unity. When one arrives at the lowest edge of the correlation rectangle to which site (i,j) belongs, all the vertical in-bonds are characterized by vanishing coefficients l' (except at row $j+k'$), whereas all the vertical out-bonds are also characterized by vanishing coefficients l' (due to the wing contribution). At site (i,j) and for the lattice configuration described by Fig. 3(b), the integral $F_{i,j}$ is reduced to the product $\cos\theta_{i,j}\, Y^*_{l_{i,j},m_{i,j}}(\mathbf{S}_{i,j})$, whereas at site $(i-1,j+k')$, i.e., at the right lower corner of the correlation rectangle, $F_{i-1,j+k'}$ contains a similar product $Y_{1,0}(\mathbf{S}_{i-1,j+k'})Y_{l_{i-1,j+k'-1},m_{i-1,j+k'-1}}(\mathbf{S}_{i-1,j+k'})$ due to the preceding work of integration. For the other edge sites each current integral $F_{K,K'}$ reduces to the product of two spherical harmonics characterizing consecutive vertical and horizontal bonds. Consequently, these integrals do not vanish if all the edge coefficients are such as $l_{\mathrm{ed}}=1$, $m_{\mathrm{ed}}=0$. In other words, the correlation path is nothing more than the respective right and lower edges of the correlation rectangle [see Fig. 3(b), case I].

Of course, a similar reasoning may be done if one considers that the upper horizontal edge [to which site $(i+k,j+k')$ belongs] is fixed. Under these conditions the correlation path appears to be constructed by means of the respective upper and left edges of the correlation rectangle [see Fig. 3(b), case II]. Moreover, to not complicate the present discussion, we have not considered a third possibility: mixing both preceding methods [see Fig. 3(c), case III]. Finally, one can note that, as for the square lattice,[16(b)] if one or both site(s) belong(s) to the lattice edge(s), the preceding reasoning prevails too so that it keeps a general character.

In conclusion, one can say that, due to the fact that the correlation rectangle is always swept in the same direction, the integration process leads to the determination of coefficients l and l' characterizing horizontal zigzags and vertical rows closer and closer to the lattice heart so that one cannot go backwards, thus forbidding the possibility of finding closed paths of correlation (i.e., loops). All the preceding results constitute *theorem 3. Due to the infinite wing contribution, (i) all the paths are equivalent inside the correlation domain; i.e., they show the same length (which is the shortest one for going from one site to another one) and involve the same number of similar bonds whatever the chosen path; (ii) the number of these bonds can be simply measured along the horizontal and vertical sides of the correlation rectangle, for the honeycomb lattice structure described by Fig. 3(a).* This result constitutes a generalization of a similar theorem derived for the 2D Heisenberg classical square lattice.[16(b)]

Finally, in the infinite-lattice limit, the Z-Z spin-spin correlation may be written as

$$\langle S^z_{i,j}S^z_{i+k,j+k'}\rangle \sim \frac{1}{3}\,(uv)^{|k'|}v^{|k|},$$

$$|k| \text{ even or odd, } |k'| \text{ even,}$$

$$\langle S^z_{i,j}S^z_{i+k,j+k'}\rangle \sim \frac{1}{3}\,\frac{1}{v}\,(uv)^{|k'|}v^{|k|},$$

$$|k| \text{ even or odd, } k' \text{ odd } (k'>0),$$

$$\langle S^z_{i,j}S^z_{i+k,j+k'}\rangle \sim \frac{1}{3}\,v(uv)^{|k'|}v^{|k|},$$

$$|k| \text{ even or odd, } k' \text{ odd } (k'<0), \quad \text{as } N\to+\infty, \tag{14}$$

where u and v are given by

$$u=\mathcal{L}(-\beta J_0), \quad v=\mathcal{L}(-\beta J), \tag{15}$$

and where $\mathcal{L}(-\beta j)$ is the well-known Langevin function.

E. Evaluation of the static susceptibility for an infinite honeycomb lattice

Due to the isotropic aspect of couplings, the static susceptibilities χ_{xx}, χ_{yy}, and χ_{zz} are equal and labeled χ; consequently, the static susceptibility per site can be defined owing to the Z-Z spin-spin correlations, i.e.,

$$\chi=\beta\sum_{k=-N}^{N}\sum_{k'=-N}^{N}G_{i,j}G_{i+k,j+k'}\langle S_{i,j}^{z}S_{i+k,j+k'}^{z}\rangle; \quad (16)$$

note that the dynamic susceptibility $\chi(q)$ can be simply derived from Eq. (16) by means of a Fourier transform—i.e., by adding the factor $\exp[-i(q_y k+q_x k')]$, where q_x and q_y are the components of the wave vector **q**. Therefore, exact knowledge of the spin-spin correlations allows one to evaluate the susceptibility. Reporting the relevant Z-Z correlation given by Eq. (14) in Eq. (16), we can define a susceptibility χ per two consecutive unit cell sites:

$$\chi=\frac{\beta}{6}\frac{(G^2+G'^2)W_1+2GG'W_2}{(1-u^2v^2)(1-v^2)} \quad \text{as} \quad N\to+\infty, \quad (17)$$

with

$$W_1=(1+uv)^2(1+v^2),$$

$$W_2=2v(1+uv)^2+u(1-v^2)^2. \quad (18)$$

At this step, one can note that, in the particular case of the chain limit ($J_0=0$, i.e., $u=0$), one finds again Fisher's result;[17] in addition, if $J=0$, i.e., $v=0$, one retrieves the well-known dimer susceptibility. As previously explained, we are mainly going to focus on the behaviors of the product χT. For practical purposes its value will be considered normalized to the infinite-temperature value (the Curie constant) so that χT will be labeled $(\chi T)_n$. Similarly, we shall introduce the ratio of magnetic moments, $r=G'/G$ (note that because of the classical character of the involved spin moments r is always equal to or lower than unity).

F. Evaluation of the correlation length for an infinite honeycomb lattice

The correlation length ξ also appears as a very useful and significant quantity from a physical point of view, notably near the critical point; it may be defined as

$$\xi=\left(\frac{\Sigma_{k=-\infty}^{+\infty}\Sigma_{k'=-\infty}^{+\infty}(k^2+k'^2)|\langle S_{0,0}^{z}S_{k,k'}^{z}\rangle|}{\Sigma_{k=-\infty}^{+\infty}\Sigma_{k'=-\infty}^{+\infty}|\langle S_{0,0}^{z}S_{k,k'}^{z}\rangle|}\right)^{1/2}. \quad (19)$$

Similarly, equivalent correlation lengths ξ_1 and ξ_2 can be defined for the horizontal zigzag ($k=0$) and the vertical lines ($k'=0$) of the lattice, respectively, characterized by the exchange energies (J_0, J) and J. Using the closed-form expression of the spin-spin correlation given by Eq. (14), we have

$$\xi_1=\left[\frac{8u^2v^2(1+u^2v^2)+u^2|v|(1+v^2)[(1+u^2v^2)^2+4u^2v^2]}{[1+|u|(1+v^2)+u^2v^2](1-u^2v^2)^2}\right]^{1/2},$$

$$\xi_2=\left[\frac{8v^2(1+v^2)+2|v|[(1+v^2)^2+4v^2]}{(1+|v|)^2(1-v^2)^2}\right]^{1/2}, \quad \xi=\sqrt{(\xi_1)^2+(\xi_2)^2}. \quad (20)$$

III. THEORETICAL DISCUSSION

A. Determination of the critical exponents

In the low-temperature range the Langevin functions $u=\mathcal{L}(-\beta J_0)$ and $v=\mathcal{L}(-\beta J)$ tend to unity (in absolute value). Therefore, the correlation lengths ξ_1 and ξ_2 defined above by Eq. (20) behave as $(1-u^2v^2)^{-1}$ and $(1-v^2)^{-1}$, respectively, i.e.,

$$\xi_1\sim\beta\frac{|J||J_0|}{|J|+|J_0|}, \quad \xi_2\sim\beta|J| \quad \text{as} \quad T\to 0. \quad (21)$$

Thus, as for the 2D Heisenberg classical square lattice, ξ_1 and ξ_2 (and subsequently ξ) diverge when the temperature tends to 0 K. In that case too, absolute zero plays the particular role of critical temperature. At this step one can note that, as for the 2D classical square lattice,[16(a)] this result can be directly obtained from the minimum value of the free energy $-k_BT\ln Z_N(0)$, where $Z_N(0)$ is given by Eq. (9). Consequently, the critical domain is quasi-infinite: The short-range order remains important, whereas the long-range one is absent, except at 0 K where it becomes preponderant and stable due to the fact that the quantum fluctuations are negligible. Subsequently, the corresponding critical exponent ν is such as $\nu=1$ and ξ behaves as T^{-1}.

This result is strictly similar to the corresponding one that we have exactly derived for the 2D Heisenberg classical square lattice,[15,16(b)] thus proving its universal character whatever the unit cell structure. At this step one can recall that, by using the renormalization group technique within a one-loop approximation, Chakravarty *et al.*[18] have obtained the result $\nu=1$ for a 2D Heisenberg quantum square lattice so that this value also appears to be independent of the quantum or classical nature of the spin moment. In addition, in the low-temperature domain, these authors have pointed out the coexistence of three regimes for the correlation length in the critical domain: The quantum disordered regime ($\nu=0$), the quantum critical regime ($\nu=1$), and the ''renormalized'' classical one ($\nu\to+\infty$). However, at $T=0$ K, a single regime prevails: The quantum critical one ($\nu=1$).

This situation corresponds to the present case upon which we have focused in this article and, as for the classical square lattice,[16(b)] a similar interpretation may be given. Thus this result gives an argument for validating the presence of quantum fluctuations near $T_c=0$ K (i.e., the true nature of the ξ behavior is exclusively conditioned by these fluctuations). Indeed, these fluctuations can be clearly explained by the

fact that the classical moments are characterized by an available energy-level density larger than for quantum spins (i.e., of quantum spin number such as $S<3/2$),[19] so that they can easily evolve between very close energy levels. In other words, due to these fluctuations, for a finite but low temperature, one can say that the lattice state is described by spin moments which are less than fully aligned. By approaching 0 K, it tends to a state characterized by more and more aligned spin moments and it appears more and more stable because these fluctuations are smaller and smaller: There is no long-range order for it is precisely destroyed by quantum fluctuations on behalf of the short-range order. But when T reaches 0 K exactly, a transition occurs: The ground state is then constituted by fully aligned spin moments and long-range order is preponderant. Therefore, from experiments carried out at finite temperatures as close as possible to absolute zero, it becomes possible to determine the nature of the ground state at $T_c=0$ K.

In the zero-temperature limit and for noncompensated spin sublattices ($G\neq G'$), the examination of Eq. (17) giving the static susceptibility χ allows one to say that χ diverges as $\beta\xi_1\xi_2$, i.e., according to a β^3 law. Thus, as for the 2D Heisenberg classical square lattice,[15,16(b)] the associated critical exponent is $\gamma=3$. In addition, χ appears as the vanishing q limit of the dynamic susceptibility $\chi(q)$ (which is the Fourier transform of χ). Near the critical temperature $T_c=0$ K, $\chi(0)$ (i.e., χ) behaves as $\beta^{2-\eta}$, which permits us to derive the critical exponent $\eta=-1$ (as for the square lattice).[15,16(b)] Consequently, Fisher's scaling law $\gamma=\nu(2-\eta)$ is fulfilled. This value can be also obtained from the low-temperature behavior of the spin-spin correlation [cf. Eq. (14)] on the one hand and owing to the corresponding one of the correlation lengths ξ_1 and ξ_2 on the other hand [cf. Eq. (21)]:

$$|\langle S^z_{0,0}S^z_{k,k'}\rangle|\rightarrow\frac{1}{3}\left[1-\frac{|k'|}{\xi_1}-\frac{|k|}{\xi_2}\right],$$

$$|k| \text{ even or odd, } |k'| \text{ even,}$$

$$|\langle S^z_{0,0}S^z_{k,k'}\rangle|\rightarrow\frac{1}{3}\left[1-\frac{|k'|}{\xi_1}-\frac{|k|-1}{\xi_2}\right],$$

$$|k| \text{ even or odd, } k' \text{ odd } (k'>0),$$

$$|\langle S^z_{0,0}S^z_{k,k'}\rangle|\rightarrow\frac{1}{3}\left[1-\frac{|k'|}{\xi_1}-\frac{|k|+1}{\xi_2}\right],$$

$$|k| \text{ even or odd, } k' \text{ odd } (k'<0), \quad \text{as } T\rightarrow 0. \quad (22)$$

The distance between sites (0,0) and (k,k') can be represented by the length of a vector the components of which are $|k'|$ and $|k|$ (respectively, $|k|-1$ or $|k|+1$) along the horizontal and vertical axes of the lattice. In the low-temperature range (i.e., near the critical point) we always have $|k'|\ll\xi_1$, $|k|\ll\xi_2$: Thus this is the deviation between unity and the ratios $|k'|/\xi_1$ and $|k|/\xi_2$ which is relevant. Consequently, for a fixed temperature near 0 K, the spin-spin correlation does globally decrease with distance (in absolute value); moreover, for a fixed distance (i.e., for fixed k and k'), it decreases according to a T law when T increases. In other words, the general power law $r^{-(D-2+\eta)}$ which describes the decay of the critical correlation is fulfilled when $\eta=-1$ and $D=2$, but this result must be handled with care because a rough interpretation could naively lead one to think that the spin-spin correlation increases with distance according to a r law, as for the classical square lattice.[16(b)]

It must be noted that a similar paradox occurs with open classical spin chains ($D=1$) showing Heisenberg-type couplings between nearest neighbors (the corresponding critical exponents are $\nu=1$, $\gamma=2$, and $\eta=0$, respectively). This aspect has been clearly detailed in a preceding article[16(b)] and is notably due to the classical aspect of the involved moments and the isotropic character of couplings.

Finally, near absolute zero (i.e., the critical temperature), the specific heat per site C behaves as

$$C\sim k_B\left[\frac{3}{2}-2(\beta J_0)^2\exp(-2\beta|J_0|)-4(\beta J)^2\right.$$
$$\left.\times\exp(-2\beta|J|)\right] \quad \text{as } T\rightarrow 0. \quad (23)$$

Thus C/k_B tends to 3/2 when the temperature tends to 0 K; the corresponding critical exponent is such as $\alpha=0$, as for the 2D Heisenberg classical square lattice.[16(b)] Therefore, Josephson's scaling law $\alpha=2-\nu D$, where D is the layer dimensionality, is fulfilled.

B. Construction of the 2D spin arrangement

In a first step and for simplifying the discussion, we exclusively consider that $|J|\gg|J_0|$. In other words, the physical study can be summarized to that of vertical classical spin chains characterized by the same exchange energy J and weakly coupled to each other by means of J_0, thus leading to a 2D arrangement [see Fig. 3(a)]. At a very high temperature, i.e., at a temperature such as $k_BT\gg|J|$, the chain behavior is dominant. If $|J|$ is weak enough, one can reach the low-temperature domain. In that case the quasi-isolated vertical chains are made of quasirigid quasi-independent blocks of length ξ_2 [where ξ_2 behaves as $\beta|J|$ near 0 K; cf. Eq. (21)]. This chain behavior is maintained down to the temperature at which the interchain exchange energy J_0 of such blocks of length ξ_2 becomes similar to k_BT. This crossover temperature T_{CO} then appears to be the solution of the following equation:

$$k_BT_{CO}\sim\xi_2|J_0|; \quad (24)$$

by means of Eq. (21), which also gives the low-temperature behavior of ξ_2, one derives

$$k_BT_{CO}\sim\sqrt{|JJ_0|}. \quad (25)$$

In the intermediate case, i.e., for closer values of J_0 and J, when $|J_0|\leqslant|J|$ or $|J_0|\geqslant|J|$, at high temperature, the lattice can be considered as an assembly of horizontal zigzag chains (characterized by the regular alternation of exchange energies J_0 and J) coupled to each other by means of bonds involving the exchange energy J. This aspect is enhanced as soon as the temperature obeys Eq. (24) in which ξ_1 is substituted for ξ_2 and J for J_0. In that case Eq. (25) giving the crossover temperature must be replaced by

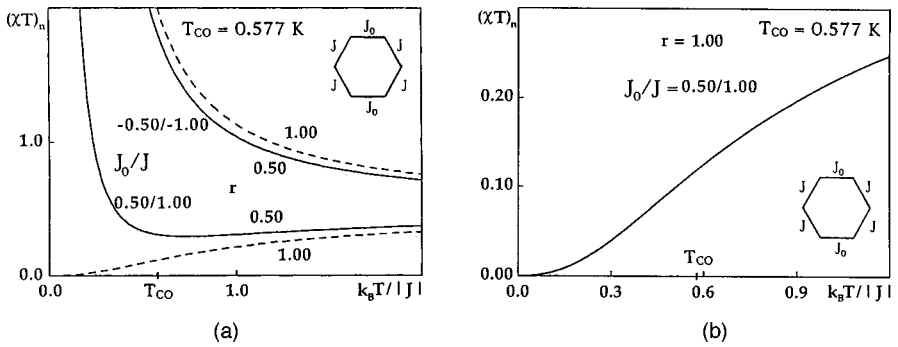

FIG. 4. Thermal behaviors of the product $(\chi T)_n$ for a honeycomb lattice composed of classical spins isotropically coupled (case $J_0 J > 0$).

$$k_B T_{CO} \sim |J| \sqrt{\frac{|J_0|}{|J|+|J_0|}}. \tag{26}$$

In a second step, if we consider that $|J| \ll |J_0|$, we deal with horizontal dimers which are weakly coupled at temperatures such as $k_B T \gg |J_0|$. When the temperature is cooling down, the intercouplings become effective if the interdimer exchange energy becomes similar to $k_B T$. In the present case the corresponding correlation length ξ_1 (expressed in lattice step units) reduces to unity [which can be directly obtained in Eq. (19) by assuming $k=0, k'=1$]. Therefore, the new crossover temperature T'_{CO} is given by the solution of the equation

$$k_B T'_{CO} \sim \xi_1 |J|, \tag{27}$$

i.e.,

$$k_B T'_{CO} \sim |J|. \tag{28}$$

In both cases, as soon as the temperature decreases from T_{CO}, the 2D arrangement becomes dominant. One must note that, for regular honeycomb lattices such as $J_0 = J$, 2D ordering already exists at high temperature and is more and more enhanced when the temperature is cooling down, i.e., as soon as $k_B T$ reaches $|J|$.

Finally, if the respective values taken by $|J_0|$ and $|J|$ do not allow one to classify T_{CO} or T'_{CO} in the low-temperature range, the problem is plainly more complicated. We always have to compare the interchain exchange energy of blocks of length ξ_1 or ξ_2 to $k_B T$ (where ξ_i, with $i=1,2$, is the correlation length corresponding to the ''dominant'' chain, i.e., the chain characterized by the strongest exchange energies). In other words, one has an equation similar to Eq. (24) or (27), but, now, ξ_2 (respectively, ξ_1) must be replaced by its temperature-dependent expression given by Eq. (20). Therefore, in that case, a numerical resolution is unavoidable.

C. Study of the low-temperature behaviors of the static susceptibility

Let $\mathcal{M}$ be the temperature-dependent magnitude of the magnetic moment per unit cell (note that $\mathcal{M}$ mainly depends on the sign of the exchange energies J_0 and J). When the temperature reaches absolute zero (i.e., the critical point) and if one considers the expression of the static susceptibility [cf. Eq. (17)], it is easily shown that the low-temperature behavior of χT is essentially ruled by that of $\xi_1 \xi_2 \mathcal{M}^2$, where $\mathcal{M}$ has been just defined above and where ξ_1 and ξ_2 are the correlation lengths associated with the horizontal and vertical lines of the lattice, respectively [cf. Eq. (21)]. Thus, in the low-temperature range, the lattice can be considered as an assembly of quasi-independent quasirigid rectangular blocks, each one being characterized by sides of respective lengths ξ_1 and ξ_2, and moment $\mathcal{M}$. Subsequently, the value of the product χT is mainly related to that of $\mathcal{M}$: If $\mathcal{M}$ is finite (noncompensated sublattices, $G \neq G'$), χT diverges as $\xi_1 \xi_2$, i.e., according to a β^2 law; if $\mathcal{M}$ vanishes in the ground state (compensated sublattices), the behavior of χT appears as a competition between the divergence of $\xi_1 \xi_2$ and the evanescence of $\mathcal{M}$.

Due to the unit cell structure involving two types of exchange energies J_0 and J, two cases of interest must be examined: If $J_0 J > 0$, the couplings J_0 and J have the same sign; i.e., they are both ferromagnetic ($J_0 < 0$, $J < 0$) or antiferromagnetic ($J_0 > 0$, $J > 0$); if $J_0 J < 0$, J_0 and J have opposite signs, so that if J_0 is ferromagnetic ($J_0 < 0$), J is antiferromagnetic ($J > 0$) and reciprocally.

In a first step, let us consider a ferromagnetic or an antiferromagnetic lattice (characterized by noncompensated sublattices, $G \neq G'$, $r \neq 1$). In other words, we have $J_0 J > 0$. Using the low-temperature behaviors of the Langevin functions u and v [defined by Eq. (15)] in the definition of the static susceptibility [cf. Eq. (17)], one derives

$$G \neq G' \quad (r \neq 1) \quad \chi T \sim \frac{\beta^2}{3} \frac{|J|^2 |J_0|}{|J|+|J_0|} \left(G - \frac{J}{|J|} G' \right)^2 \quad \text{as } T \to 0. \tag{29}$$

Thus, as expected, χT diverges according to a β^2 law due to the fact that the magnetic moment $\mathcal{M}$, i.e., $G \pm G'$, is finite in the ground state. In addition, the divergence is accentuated for ferromagnetic couplings ($J_0 < 0$, $J < 0$) due to the fact that the magnitude of $\mathcal{M}$ is more important than in the antiferromagnetic case ($J_0 > 0$, $J > 0$). These behaviors are reported in Fig. 4(a) ($|J_0|/k_B = 0.50$ K, $|J|/k_B = 1.00$ K); under these

conditions, the crossover temperature T_{CO} [given by Eq. (26)] is such as $T_{CO}=0.577$ K. In this respect one can note that the divergence of χT is plainly accentuated for ferromagnetic or antiferromagnetic lattices when T_{CO} is reached due to the fact that the 2D ordering becomes effective, thus characterizing the fact that the lattice moment is more important. For compensated sublattices ($J_0>0$, $J>0$, $G=G'$, $r=1$), the factor $G-G'$ in Eq. (29) vanishes near the critical point (i.e., 0 K) and the T expansion must be examined up to the following term; one has

$$J_0>0, \quad J>0, \quad G=G' \quad (r=1),$$

$$\chi T \rightarrow \frac{G^2}{12J_0J}\,\frac{2J_0+J}{J_0+J}\,(k_BT)^2 \quad \text{as} \quad T\rightarrow 0. \tag{30}$$

In the present case, as $J_0<J$, we deal with vertical compensated chains at temperatures such as $k_BT>|J|$; when T_{CO} is reached (i.e., 0.577 K), a change of slope is duly observed: The product χT vanishes according to a T^2 law instead of a T one, for similar isolated vertical chains [see Fig. 4(b)]. As χT behaves as $\xi_1\xi_2\mathcal{M}^2$, i.e., as $\beta^2\mathcal{M}^2$ in the low-temperature range, one derives that $\mathcal{M}$ vanishes according to a T^2 law.

If $J_0J<0$, the horizontal and vertical bonds of the lattice are characterized by exchange energies showing opposite signs. By assuming a similar work that in the case $J_0J>0$, we derive, in the low-temperature range,

$$\chi T \rightarrow \frac{1}{12}\left[\alpha\left\{\frac{2+\alpha}{1+\alpha}+\frac{(\alpha-1)(\alpha^2+2\alpha+2)}{2|J|(1+\alpha)^2}\,k_BT\right\}\times\left(G-\frac{J}{|J|}\,G'\right)^2+\left\{\frac{1}{1+\alpha}-\frac{\alpha-1}{2|J|(1+\alpha)^2}\,k_BT\right\}\times\left(G+\frac{J}{|J|}\,G'\right)^2\right],$$

$$\alpha=\left|\frac{J}{J_0}\right| \quad (\alpha\neq 1), \quad \text{as} \quad T\rightarrow 0, \tag{31}$$

$$\chi T \rightarrow \frac{1}{12}\left[\left\{\frac{3}{2}-\frac{29}{8J^2}\,(k_BT)^2\right\}\left(G-\frac{J}{|J|}\,G'\right)^2+\left\{\frac{1}{2}-\frac{17}{8J^2}\,(k_BT)^2\right\}\left(G+\frac{J}{|J|}\,G'\right)^2\right],$$

$$\alpha=1, \quad \text{as} \quad T\rightarrow 0. \tag{32}$$

In all cases the infinite lattice shows a vanishing moment in the ground state. In other words, as χT always tends to a constant limit near the critical point, that means that the magnetic moment $\mathcal{M}$ vanishes according to a T law. If the horizontal couplings are antiferromagnetic ($J_0>0$) and the vertical ones ferromagnetic ($J<0$), the horizontal zigzags are made of antiferromagnetic pairs of spins ferromagnetically coupled (case I). If $|J_0|<|J|$, at low temperature, the dominant vertical rows are made of ferromagnetic chains ($J<0$) antiferromagnetically coupled ($J_0>0$), whereas if $|J_0|>|J|$, one deals with dominant alternated horizontal zigzags ferromagnetically coupled ($J<0$). Subsequently, the ratio $r=G'/G$ loses its specific character with respect to the problem of compensation between consecutive sites of the same unit cell. In other words, if $|J_0|<|J|$, the vertical ferromagnetic chains carry a stronger moment than in the case $|J_0|>|J|$. Therefore, the corresponding value of χT is always greater [see Figs. 5(a) and 5(b)]. When T_{CO} is reached the 2D ordering becomes effective. A change of behavior is duly observed and is more accentuated if $|J_0|<|J|$ due to the fact that we deal with a phenomenon of compensation between consecutive ferromagnetic vertical chains. In these two cases and whatever the value of $r=G'/G$, χT tends to a constant limit according to a T law with a positive ($|J_0|<|J|$) or a negative ($|J_0|>|J|$) slope. This character can be simply derived in Eq. (31) by assuming $J/|J|=-1$ and $G=G'$ ($r=1$). If $G\neq G'$ ($r\neq 1$), a numerical study is necessary, but from a physical point of view, as the ratio $r=G'/G$ has lost its specific influence, one can predict that the behavior of χT is not drastically changed. This aspect is confirmed by a comparison of the corresponding curves of Figs. 5(a) and 5(b). In the particular case $J_0=-J$, the low-temperature expansion of χT given by Eq. (31) must be replaced by that given by Eq. (32). Near 0 K, χT also tends to a constant limit, but now with a T^2 law. This is due to the fact that we deal with the double compensation between consecutive vertical ferromagnetic chains on the one hand and horizontal antiferromagnetic spin pairs on the other hand.

If the horizontal couplings are ferromagnetic ($J_0<0$) and the vertical ones antiferromagnetic ($J>0$), the horizontal zigzags are made of ferromagnetic pairs of spins antiferromagnetically coupled. In other words, if $|J_0|<|J|$, we deal with dominant vertical antiferromagnetic chains ($J>0$) ferromagnetically coupled ($J_0<0$), whereas if $|J_0|>|J|$, we still have dominant alternated horizontal zigzags antiferromagnetically coupled to each other. Therefore, in all cases, the global magnetic moment involved in the case $J_0<0$, $J>0$ (case II) is always lower than the corresponding one in the case $J_0>0$, $J<0$ (case I). Thus one can predict two consequences: (i) For a given ratio $\alpha=|J/J_0|$, χT is always lower in case II than in case I; (ii) χT decreases when α increases in case II, whereas it increases with α in case I. These phenomena can be easily observed in Figs. 5(c) and 5(d) on the one hand and by comparing Figs. 5(a) and 5(c) as well as Figs. 5(b) and 5(d) on the other hand. Subsequently the interpretation of the χT curves in case II is very similar to that one given above in case I. However, a slight difference occurs in the present case II: Due to the fact that χT shows smaller values than in case I, the ratio $r=G'/G$ has a smaller influence over the χT slope near 0 K.

IV. COMPARISON WITH EXPERIMENTAL RESULTS

A. General considerations

In a preceding article concerning the 2D Heisenberg classical square lattice,[16(c)] we have recalled the general conditions which must be fulfilled by the magnetic ions and the various ligands involved for obtaining a quasi-2D lattice characterized by isotropic couplings. Notably, we have noticed that the ion Mn^{2+} is an excellent candidate. Thus, for Heisenberg-type couplings, the three static susceptibilities, respectively, measured along the three axes *a*, *b*, and *c* of the

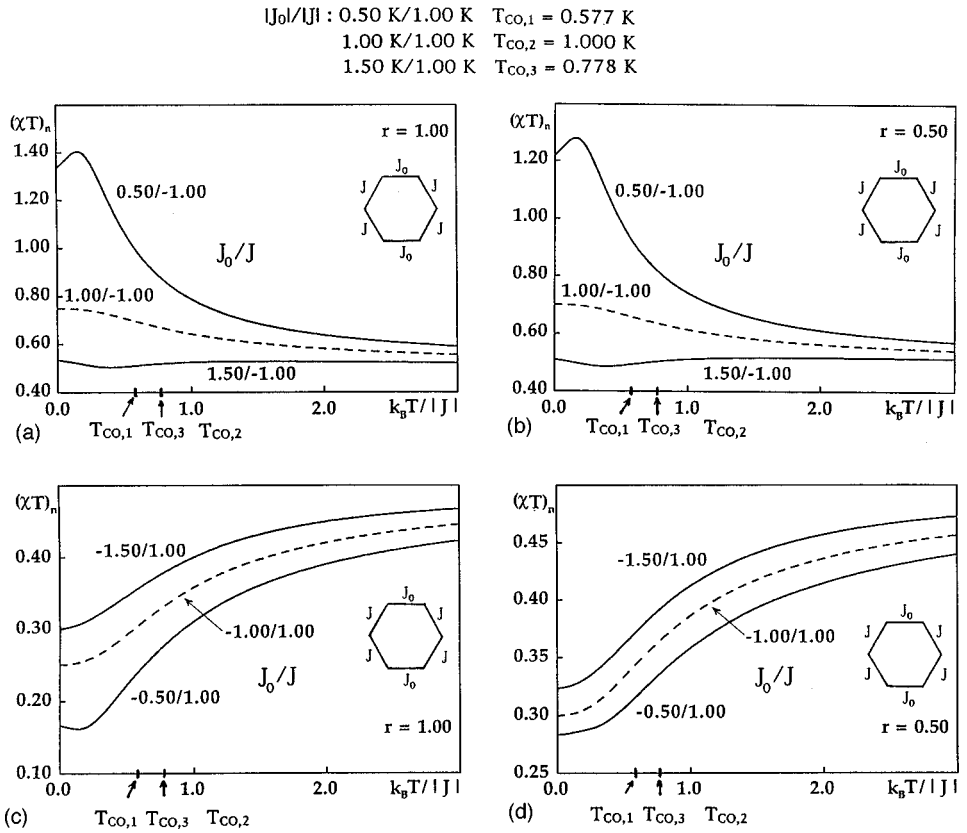

FIG. 5. Thermal behaviors of the product $(\chi T)_n$ for a honeycomb lattice composed of classical spins isotropically coupled (case $J_0 J < 0$).

crystal, i.e., χ_a, χ_b, and χ_c, are equal to a common value χ. More particularly, for compensated antiferromagnetic compounds, the susceptibility curve shows a maximum which appears as a characteristic signature of such a kind of magnetic behavior. When the temperature is still cooling down, χ vanishes according to a T law [cf. Eq. (30)] if one deals with a purely 2D lattice. But as often occurs, if the lattice is not a purely 2D one, the three-dimensional magnetic ordering appears at the Néel temperature T_N.

Above T_N, by coming from the high-temperature domain, χ_a, χ_b, and χ_c remain equal to χ and gradually increase up to a characteristic maximum before decreasing. When T_N is reached, generally χ_a and χ_b remain equal (otherwise, one deals with an anisotropic compound) and are labeled $\chi_\parallel$ (parallel susceptibility); then, below T_N, $\chi_\parallel$ rapidly decreases with temperature before vanishing at 0 K, as expected for an antiferromagnet. As for the out-plane contribution χ_c (or perpendicular susceptibility $\chi_\perp$), it passes through a minimum value at T_N and slightly increases before tending to a constant value at 0 K. At this step, one can give an estimate of T_N. In the low-temperature range, as previously seen in Sec. III B, the lattice is made of quasi-independent quasirigid blocks, the sides of which have the respective lengths ξ_1 and ξ_2, i.e., the correlation lengths associated with the horizontal zigzags and the vertical lines of the lattice. If J' is the interlayer exchange energy, the 3D magnetic ordering appears when the interlayer energy of blocks of surface $\xi_1 \xi_2$ becomes similar to $k_B T$, i.e.,

$$k_B T \sim \xi_1 \xi_2 |J'|. \tag{33}$$

Using the low-temperature expression of ξ_1 and ξ_2 [cf. Eq. (21)], one derives

$$k_B T \sim |J| \left(\frac{(|J'/J|)(|J_0/J|)}{1+|J_0/J|} \right)^{1/3}. \tag{34}$$

Note that T_N vanishes with J', i.e., when the arrangement is a purely 2D one; of course, from a practical point of view, one must not forget that the superexchange mechanism as well as the unavoidable interlayer dipolar interactions often give a further contribution to the interlayer exchange energy J'.

B. Study of the maximum of the susceptibility curve

As noted above, the study of this maximum is fundamental and we are going to show that it allows one to characterize the 2D Heisenberg magnetic behavior. In this respect, one can easily guess that this characterization will be excellent if the Néel temperature T_N and the temperature of the maximum $T(\chi_{\max})$ are well separated. By replacing J_0 and J with their respective renormalized expressions $j_0 = J_0 S(S+1)$ and $j = JS(S+1)$ (with $S = 5/2$) and by derivating the susceptibility χ [given by Eqs. (17) and (18)] with respect to the temperature, one has to solve the following equation:

$$u' A + v' B - C = 0, \tag{35}$$

with

$$u' = \beta j_0 (1 - \coth^2(\beta j_0)) + \frac{1}{\beta j_0},$$

$$v' = \beta j[1-\coth^2(\beta j)] + \frac{1}{\beta j},$$

$$A = \{[1+v^2(1+2u)](1-u^2v^2) + 2uv^2(1+uv^2)(1+u)\} \times (1-v^2),$$

$$B = \{[1+uv(2+3v)](1-u^2v^2)(1-v) + [1+u^2v(2-3v)] \times (1+uv^2)(1+v)\}(1+u),$$

$$C = (1+uv^2)(1-u^2v^2)(1+u)(1-v^2), \tag{36}$$

where u and v are the respective Langevin functions $\mathcal{L}(-\beta J_0)$ and $\mathcal{L}(-\beta J)$.

Of course, Eq. (35) can only be solved numerically and, for given j_0/k_B and j/k_B, one may derive the temperature $T(\chi_{\max})$ of the maximum of the susceptibility curve. For simplifying the discussion, in a first step, we exclusively consider that $J_0 = J$. We have found

$$k_B T(\chi_{\max}) = 1.0648j, \quad j = JS(S+1), \quad S = 5/2. \tag{37}$$

This study has been previously achieved for a 2D Heisenberg classical square lattice,[16(c)] and we have derived that the corresponding coefficient is 1.2625, which is very close to the value published by Lines[20] and later by De Jongh and Miedema[1,21] after having fitted experimental susceptibilities owing to refined high-temperature (HT) series expansions. In other words, such a kind of coefficient appears as a universal constant characterizing the nature of the unit cell. Thus knowledge of $T(\chi_{\max})$ allows one to derive the exchange energy J.

But from a practical point of view and as remarked by De Jongh and Miedema,[1,21] the susceptibility curves often show a broad maximum so that the corresponding temperature $T(\chi_{\max})$ is known with a poor accuracy. Therefore, it is more interesting to study the inverse of the value of the susceptibility. Under these conditions, we have derived

$$\frac{G^2}{\chi_{\max}} = 8.5117j, \quad j = JS(S+1), \quad S = 5/2. \tag{38}$$

For the 2D Heisenberg classical square lattice,[16(c)] we have found 10.6838. Another quantity which often appears in the literature is the ratio $\chi_{\max}T(\chi_{\max})/C$, where C is the Curie constant (i.e., $G^2/3k_B$ in our case if one considers the susceptibility per atom). We have obtained

$$\frac{\chi_{\max}T(\chi_{\max})}{C} = 0.3753. \tag{39}$$

In that case too, this coefficient exclusively characterizes the hexagonal unit cell and thus shows a universal character (for the 2D Heisenberg classical square lattice, we have derived the value 0.3545, which is also very close to that one obtained by De Jongh and Miedema owing to HT expansions).[1,21] Finally, note that all the coefficients appearing in Eqs. (37)–(39) have been calculated with an accuracy plainly lower than 0.01%.

In a second step, one may focus on a more general case, i.e., that one concerning 2D lattices characterized by two exchange energies J_0 and J. A similar numerical study has allowed one to find the following equations:

$$k_B T(\chi_{\max}) = aj_0 + b\sqrt{j_0 j} + cj, \quad j_0 = J_0 S(S+1),$$

$$j = JS(S+1), \quad S = 5/2,$$

$$a = 0.2559, \quad b = 0.3780, \quad c = 0.4309, \tag{40}$$

$$\frac{G^2}{\chi_{\max}} = a'j_0 + b'\sqrt{j_0 j} + c'j,$$

$$a' = 2.9845, \quad b' = 0.6161, \quad c' = 4.9111, \tag{41}$$

$$\frac{\chi_{\max}T(\chi_{\max})}{C} = 3\frac{aj_0 + b\sqrt{j_0 j} + cj}{a'j_0 + b'\sqrt{j_0 j} + c'j}. \tag{42}$$

Of course, one can note that, when $j_0 = j$, one retrieves the respective results of Eqs. (37)–(39). Consequently, we have plotted $T(\chi_{\max})$, $G^2/\chi_{\max}$, and $\chi_{\max}T(\chi_{\max})/C$ versus j_0/k_B and j/k_B; they are, respectively, illustrated by Figs. 6(a), 6(b), and 6(c). The linear behaviors of $T(\chi_{\max})$ and $G^2/\chi_{\max}$ have been also reported when $J_0 = J$. Thus, under these conditions, one may derive the respective values of J_0 and J. Using Eq. (42) and setting

$$\alpha = \frac{J}{J_0}, \quad \tau = \frac{\chi_{\max}T(\chi_{\max})}{C}, \tag{43}$$

one has to solve

$$(c - c'\tau)\alpha + (b - b'\tau)\sqrt{\alpha} + (a - a'\tau) = 0, \tag{44}$$

where a, a', b, b', c, and c' are given by Eqs. (40) and (41). A numerical study has allowed one to show that the convenient root is

$$\sqrt{\alpha} = \frac{-(b - b'\tau) - \sqrt{(b - b'\tau)^2 - 4(a - a'\tau)(c - c'\tau)}}{2(c - c'\tau)}, \tag{45}$$

so that

$$\frac{J_0}{k_B} = \frac{G^2/\chi_{\max}}{a' + b'\sqrt{\alpha} + c'\alpha}, \quad \frac{J}{k_B} = \frac{\alpha G^2/\chi_{\max}}{a' + b'\sqrt{\alpha} + c'\alpha}. \tag{46}$$

Note that similar expressions can be derived from knowledge of $T(\chi_{\max})$ owing to Eq. (40). A further numerical study concerning the comparison between the initially imposed values of J_0 and J leading to the numerical results of $T(\chi_{\max})$, $G^2/\chi_{\max}$, and $\chi_{\max}T(\chi_{\max})/C$ and the corresponding values derived from Eq. (46) has been achieved. If $J > J_0$ or J slightly lower than J_0, J is obtained with an accuracy lower than 1%; α and J_0 are given with a precision lower than 5% if α is such as $0.8 \leqslant \alpha \leqslant 12.5$ (respectively, 6.4% if $\alpha \leqslant 14$, 8% if $\alpha \leqslant 16$, and 10% if $\alpha \leqslant 18.5$). Thus, *a posteriori*, we can justify the choice of Eq. (42) for finding α by the fact according to which its expression given by the root of Eq. (44) limits the cumulative products of coefficients a, a', b, b', c, and c' and plainly improves the accuracy with

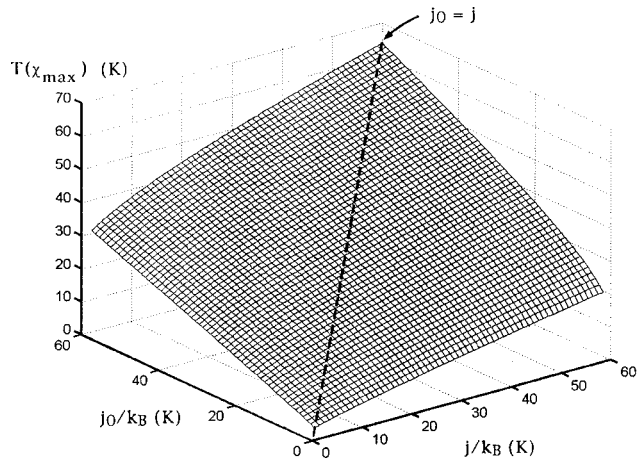

$j_0 \neq j \quad k_B T(\chi_{max}) = aj_0 + b\sqrt{j_0 j} + cj$

$a = 0.2559 \quad b = 0.3780 \quad c = 0.4309$

$j_0 = j \quad k_B T(\chi_{max}) = (a + b + c)\, j_0$

$a + b + c = 1.0648$

(a)

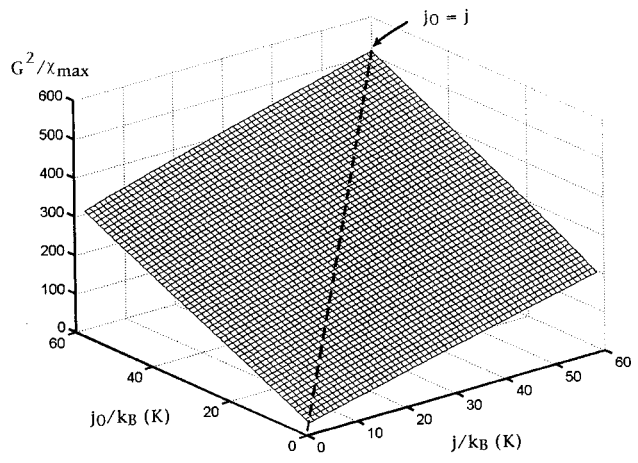

$j_0 \neq j \quad G^2/\chi_{max} = a'j_0 + b'\sqrt{j_0 j} + c'j$

$a' = 2.9845 \quad b' = 0.6161 \quad c' = 4.9111.$

$j_0 = j \quad G^2/\chi_{max} = (a' + b' + c')j_0$

$a' + b' + c' = 8.5117$

(b)

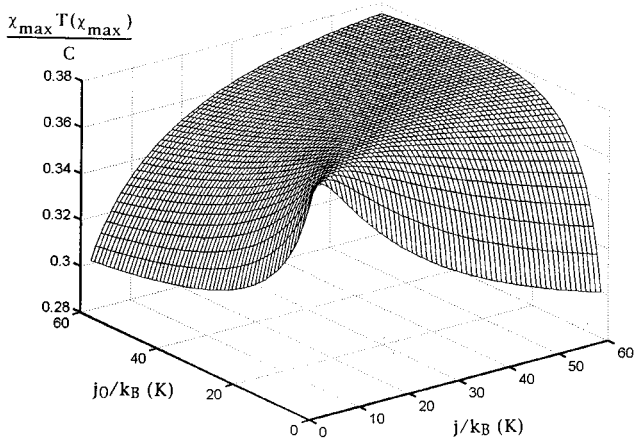

$$j_0 \neq j \quad \frac{\chi_{max} T(\chi_{max})}{C} = 3\frac{aj_0 + b\sqrt{j_0 j} + cj}{a'j_0 + b'\sqrt{j_0 j} + c'j}, \qquad C = \frac{G^2}{3k_B}$$

$$j_0 = j \quad \frac{\chi_{max} T(\chi_{max})}{C} = 0.3753$$

(c)

FIG. 6. (a) Variation of the temperature of the maximum of the susceptibility curve $T(\chi_{max})$ versus the exchange energies j_0/k_B and j/k_B, for a compensated 2D Heisenberg classical hexagonal lattice antiferromagnet [with $j_0 = J_0 S(S+1)$, $j = JS(S+1)$, $S = 5/2$], (b) variation of G^2/χ_{max}, and (c) variation of $\chi_{max} T(\chi_{max})/C$ where C is the Curie constant $G^2/3k_B$.

which J_0 and J are found. In this respect, by combining Eqs. (40) and (41), we have verified that the ratio α is obtained with a very poor accuracy.

In summary, the experimental determination of $T(\chi_{max})$ and G^2/χ_{max} allows one to derive directly the exchange energies J_0 and J. If $\chi_{max} T(\chi_{max})/C = 0.3753$, where the Curie constant C can be obtained from the HT experimental limit of the product χT, the 2D Heisenberg classical hexagonal lattice is characterized by a single exchange energy $J_0 = J$, which can be found owing to Eq. (37) or (38). On the contrary, if $\chi_{max} T(\chi_{max})/C \neq 0.3753$, the theoretical treatment of the maximum of the susceptibility curve just detailed above permits one to assert that the hexagonal lattice is characterized by two exchange energies J_0 and J, which can be then found owing to Eqs. (45) and (46). Thus, before testing all the experimental data with the theoretical expression of the

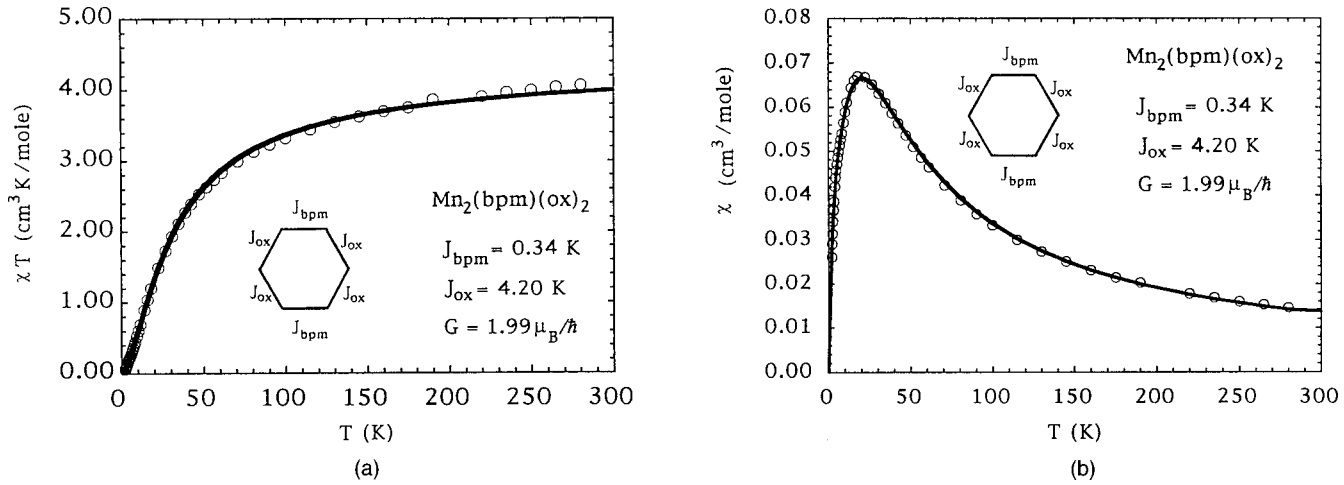

FIG. 7. (a) Fit of the experimental thermal variations of the product χT for a powder of the antiferromagnet $Mn_2(bpm)(ox)_2$ characterized by a 2D Heisenberg classical hexagonal lattice (''bpm'' and ''ox'' are the ligands bipyrimidine and oxalate) and (b) fit of the experimental thermal variations of the susceptibility χ.

susceptibility given by Eqs. (17) and (18), one may have a good estimate of the exchange energies J_0 and J. However, from an experimental point of view, one must suppose that there exist enough experimental points around the maximum of the susceptibility curve for obtaining $T(\chi_{max})$ with a correct accuracy.

C. Interpretation of the experimental data obtained for the antiferromagnet $Mn_2(bpm)(ox)_2 \cdot 6H_2O$

The variable-temperature magnetic susceptibility data (per manganese atom) have been obtained between 2 and 300 K for a powder of the complex $Mn_2(bpm)(ox)_2 \cdot 6H_2O$ (''bpm'' and ''ox'' refer to the bipyrimidine and oxalate ligands, respectively). Note that these data have been corrected for the presence of a small amount (i.e., about 1%) of paramagnetic impurities and the experimental uncertainty has been estimated to 0.1%. At first sight, the global shapes of both χT and χ curves, respectively depicted in Figs. 7(a) and 7(b), allow one to derive several important conclusions.

(i) In the high-temperature limit, the χT curve shows a plateau and the corresponding constant value at room temperature is 4.06 $cm^3\,K\,mol^{-1}$, as expected for a single ion characterized by a sextuplet. In other words, that means that we deal with a spin such as $S=5/2$ so that it can be considered as a classical one; the corresponding Landé factor is $G=2\mu_B/\hbar$, and the Curie constant is $C=4.06$ $cm^3\,K\,mol^{-1}$.

(ii) In the low-temperature range, near absolute zero, χ and χT vanish with temperature. This property is characteristic of the occurrence of antiferromagnetic couplings. As the magnetic data have been obtained on a powder sample, it means that the Néel temperature T_N is very close to 0 K; thus, one can consider that there is no three-dimensional magnetic perturbation. Otherwise, as explained in Sec. IV A, below T_N, the perpendicular contribution to the susceptibility, i.e., $\chi_\perp$, tends to a constant limit at 0 K so that, globally, the total susceptibility does not vanish too. Therefore, one can immediately derive that the antiferromagnetic couplings are isotropic for $T \geqslant 2$ K. At this step, one can recall that, for open compensated Heisenberg classical spin chains, χ tends to a constant limit at 0 K, whereas χT vanishes according to a T law.[17] For a 2D-compensated Heisenberg classical honeycomb lattice, we have shown that χ vanishes according to a T law, while χT vanishes according to a T^2 law [cf. Eq. (30)]. In the present experimental case, χ and χT vanish simultaneously, notably with a T law for the total susceptibility χ. Thus, starting from the crystallographic structure depicted by Fig. 1, all the information given in points (i) and (ii) allows one to conclude that, from a magnetic point of view, the compound $Mn_2(bpm)(ox)_2 \cdot 6H_2O$ is well described by a 2D Heisenberg classical honeycomb lattice, thus justifying the arguments detailed in the Introduction of the present article.

(iii) In order to be definitively sure, let us examine the characteristic maximum of the susceptibility curve illustrated by Fig. 7(b). More refined measurements (i.e., more experimental points obtained around the maximum) give a good determination of χ_{max} and $T(\chi_{max})$. Note that this work is facilitated by the fact that the susceptibility curve maximum is not too broad. Under these conditions, we have exactly found $\chi_{max}=6.697\times10^{-2}$ $cm^3\,mol^{-1}$ and $T(\chi_{max})=20.5$ K. We immediately derive that $\chi_{max}T(\chi_{max})/C=0.3381$, where C has been given above. Consequently, as $\chi_{max}T(\chi_{max})/C \neq 0.3753$, this experimental result confirms that the 2D classical honeycomb structure is characterized by two different exchange energies J_0 and J. Comparing with the structure of the compound $Mn_2(bpm)(ox)_2 \cdot 6H_2O$ depicted by Fig. 1 on the one hand and the theoretical convention used for describing the unit cell on the other hand, one can set $J_{bpm}=J_0$ and $J_{ox}=J$. At this step, one must recall that the comparison between the experimental molar susceptibility per atom of manganese(II) and the theoretical expression of the susceptibility derived from our model [cf. Eq. (17) in which one considers equal Landé factors G and G'] imposes to renormalize the theoretical susceptibility by the factor $\mathcal{N}\mu_B{}^2S(S+1)/k_B$ where $\mathcal{N}$ is the Avogadro constant, μ_B the Bohr magneton, and k_B the Boltzmann constant [the factor $S(S$

+1), with here $S=5/2$, comes from the renormalization of the Landé factor]. Under these conditions, if the experimental susceptibility is expressed in $cm^3\,mol^{-1}$, one has $\mathcal{N}\mu_B{}^2S(S+1)/k_B=3.2841$. Then, owing to Eqs. (45) and (46), which directly give the value of the exchange energies J_0/k_B and J/k_B characterizing the 2D classical honeycomb lattice when $T(\chi_{max})$ and χ_{max} are known, one may derive $J_{bmp}/k_B=0.32$ K and $J_{ox}/k_B=4.22$ K if one imposes $G=2\mu_B/\hbar$. In this respect, it now becomes easy to verify that, as noticed in Sec. IV B, the experimental determination of $T(\chi_{max})$ with a good accuracy is fundamental and plainly conditions the quality of the results concerning J_{bmp} and J_{ox}. For example, if $T(\chi_{max})=20.0$ K, $J_{bmp}/k_B=0.23$ K and $J_{ox}/k_B=4.30$ K, whereas if $T(\chi_{max})=21.0$ K, $J_{bmp}/k_B=0.44$ K and $J_{ox}/k_B=4.13$ K. However, these results show that, in all cases, $J_{ox}\gg J_{bpm}$, which is in agreement with the fact that the oxalato bridge has a greater ability to transmit electronic effects. Indeed, one can recall that, for bpm-bridged manganese(II) complexes characterized by a chain structure, it has been previously found that $J_{bmp}/k_B=1.44$ K,[10,14(c),14(d)] whereas for ox-bridged manganese(II) compounds, $J_{ox}/k_B=3.45$ K.[14(a),14(b)]

Finally, owing to a refined least-squares method which allows one to optimize the parameters G, J_{bmp}, and J_{ox}, one can derive the best fit of the experimental points through the theoretical expression of the susceptibility χ given by Eqs. (17) and (18) and the product χT. Let us recall that G, J_{bmp}, and J_{ox} (i.e., J_0 and J) are renormalized by the factor $S(S+1)$, with $S=5/2$. These fits are reported in Fig. 7(a) for χT and in Fig. 7(b) for χ (solid lines). One can easily observe that all the experimental points between 2 and 300 K belong to the theoretical curve, and we have obtained $G=(1.992\pm0.002)\mu_B/\hbar$, $J_{bmp}/k_B=(0.3400\pm0.0003)$ K, and $J_{ox}/k_B=(4.200\pm0.004)$ K. Within the experimental uncertainty range, the G value derived from the fit is in perfect agreement with the corresponding theoretical one, i.e., $2\mu_B/\hbar$. In addition, the values of the exchange energies J_{bmp}/k_B and J_{ox}/k_B are also very close to the corresponding ones calculated from Eqs. (45) and (46), i.e., $J_{bmp}/k_B=0.32$ K and $J_{ox}/k_B=4.22$ K. Therefore, one can say that the theoretical expression giving the susceptibility of the 2D Heisenberg classical honeycomb lattice allows an excellent characterization of the magnetic behavior of the compound $Mn_2(bpm)(ox)_2\cdot 6H_2O$. At this step, one can notice that, by comparing these values with the corresponding ones measured for similar ligands involved in chain structures,[10,14] one can observe that the strongest exchange energy, i.e., J_{ox}, is enhanced, whereas the smallest one, i.e., J_{bpm}, is weakened. This phenomenon can be simply explained by the fact that the two-dimensional character of the lattice favors the electronic exchanges between nearest neighbors of the same lattice row showing the strongest exchange (characterized by the ox ligands) to the detriment of the lateral bonds showing the weakest one (characterized by the bpm ligands).

V. CONCLUSION

In this paper we have generalized a theoretical model previously published[15,16] in which we have set on general methods for establishing closed-form expressions of the zero-field partition function $Z_N(0)$, the specific heat, the spin-spin correlations, the static susceptibility χ, and the correlation length of a 2D Heisenberg classical square lattice. In the present case we have adapted these methods for deriving the respective expressions of the same thermodynamic functions, for a similar 2D lattice showing a hexagonal unit cell conveniently described by two different exchange energies. Then we have achieved a theoretical study of the low-temperature behaviors: It has allowed us to verify that absolute zero plays the important role of critical temperature as it occurs each time that the involved spin couplings characterizing the 2D lattice are of Heisenberg type.

Near 0 K we have notably derived the critical exponents $\alpha=0$, $\eta=-1$, $\gamma=3$, and $\nu=1$ as for the 2D Heisenberg square lattice, thus confirming their universal value, independently of the nature of the involved unit cell. Similarly, in the low-temperature range, we have shown that the product χT behaves as $\xi_1\xi_2\mathcal{M}^2$ where ξ_1 and ξ_2 are the correlation lengths associated with the infinite horizontal and vertical lattice lines and $\mathcal{M}$ the temperature-dependent magnitude of the magnetic moment per unit cell. In other words, in the low-temperature range, the lattice is composed of quasi-independent quasirigid rectangular blocks of lengths ξ_1 and ξ_2 and moment $\mathcal{M}$. For noncompensated sublattices, χT behaves as $\xi_1\xi_2$, i.e., as β^2; for compensated sublattices, the χT behavior appears as a competition between the divergence of $\xi_1\xi_2$ and the evanescence of $\mathcal{M}$ according to a T-polynomial law which has been derived in each relevant case.

From a practical purpose, as there exit compensated 2D Heisenberg antiferromagnets, we have studied the maximum of the susceptibility curve because it gives a nonambiguous characterization of the corresponding magnetic behavior. If $T(\chi_{max})$ and χ_{max} are the respective coordinates of the maximum of the susceptibility curve and C the Curie constant, we have shown that the ratio $\chi_{max}T(\chi_{max})/C$ immediately allows one to say if the 2D Heisenberg classical honeycomb lattice is characterized by a single exchange energy J or by two ones J_0 and J [cf. Eq. (39)]. If a single exchange energy J is involved, we have shown that there is a linear variation between J/k_B and $T(\chi_{max})$ on the one hand as well as between J and G^2/χ_{max} on the other hand [cf. Eqs. (37) and (38)]. If there are two exchange energies J_0 and J, we have obtained more complicated relations [cf. Eqs. (40) and (41)]. But in both cases, knowledge of $T(\chi_{max})$ and χ_{max} allows one to derive the value of the involved exchange energies so that one can simultaneously characterize (i) the isotropic aspect of couplings and (ii) the hexagonal nature of the unit cell.

For illustrating this theoretical work we have analyzed the magnetic behavior of the Heisenberg-compensated antiferromagnet $Mn_2(bpm)(ox)_2\cdot 6H_2O$, the structure of which is a 2D classical honeycomb lattice (cf. Fig. 1). This new class of 2D compound is characterized by organic ligands so that their presence allows one to distance the magnetic ions within the layer itself as well as the layers along the c axis, thus conferring on them a quasi-2D structure characterized by a Néel temperature very close to absolute zero. We have shown that, by fitting the experimental data, the curve obtained from the theoretical expression of the static susceptibility joins all the experimental points in a very broad range of temperature, whereas so far numerous models have only given approxi-

mated descriptions.[10] In addition, from the theoretical study of the characteristic maximum of the susceptibility curve, we have verified that it is possible to obtain the value of the corresponding exchange energies. In addition there are very close to the values derived by fitting all the experimental points. By comparing these values with those measured for similar ligands involved in chain structures, we have observed that the strongest exchange energy is enhanced, whereas the smallest one is weakened. As has been explained, this phenomenon results from the two-dimensional character of the lattice. Finally, because of the absence of experimental data in the very low-temperature domain, we have not been able to derive the critical exponent γ. However, for compensated 2D lattices, if it is possible to obtain these data, one can hope that the fit of the thermal variations of the static susceptibility will give an excellent method for deriving the experimental value of the critical exponent γ with a good accuracy.

ACKNOWLEDGMENT

Centre de Physique Moléculaire Optique et Hertzienne is U.M.R. 5798 Université Bordeaux I-CNRS. Partial financial support from the European Community (TMR Programme) through Contract No. ERBFM-RXCT980181 is gratefully acknowledged.

APPENDIX

We start from the characteristic polynomial of the zero-field partition function $Z_N(0)$ given by Eq. (7). In the main text we have evoked a numerical property of the functions λ_l, i.e., $(\pi/2\beta j)^{1/2} I_{l+1/2}(-\beta j)$, which decrease when l increases, for the same nonvanishing argument βj. Therefore, the term of higher degree is obtained when all the $l_{i,j}$'s and all the $l'_{i,j}$'s are equal to a common positive (or null) value l, for the whole lattice. Thus all the l and l' summations involved in Eq. (7) (and within which there exist imbricated integrals over the various spherical harmonics) reduce to a single one so that the corresponding term is $[\lambda_l(-\beta J_0)\lambda_l(-\beta J)^2]^{N(2N+1)}\lambda_l(-\beta J)^{-2}$. Note that the total superscript of the latter factor (as well as for each current term of the characteristic polynomial) represents the total number of bonds composing the honeycomb lattice, i.e., $3N(2N+1)-2$.

Now we examine second-rank terms of the characteristic polynomial; notably, the main problem concerns the determination of the upper term among all these terms of lower degree. Subsequently, we are led to distinguish the $4(3N-1)$ edge bonds characterized by the set $\{l_{\rm ed}\}$ of the various coefficients $l_{i,j}$ and $l'_{i,j}$ and the $3N(2N-3)+2$ inside bonds characterized by the *same* coefficients $l_{i,j}$ and $l'_{i,j}$ labeled $l_{\rm in}$. The edge contribution is labeled $\Lambda^{\rm ed}_{\{l_{\rm ed}\}}$, and it involves the product of $4(3N-1)$ functions $\lambda_l(-\beta j)$, i.e., $4N$ functions $\lambda_l(-\beta J_0)$ and $4(2N-1)$ functions $\lambda_l(-\beta J)$; the in-contribution is $(\Lambda^{\rm in}_{l_{\rm in}})^{N(2N-3)}\lambda_{l_{\rm in}}(-\beta J)^2$ with $\Lambda^{\rm in}_{l_{\rm in}} = \lambda_{l_{\rm in}}(-\beta J_0)\lambda_{l_{\rm in}}(-\beta J)^2$. In this respect, note that the term of higher degree can be also expressed as the product $(\Lambda^{\rm ed}_l)^{4N}(\Lambda^{\rm in}_l)^{N(2N-3)}\lambda_l(-\beta J)^{-2}$, with $\Lambda^{\rm ed}_l = \Lambda^{\rm in}_l = \Lambda^{\rm in}_{l_{\rm in}}$, for $l_{\rm ed} = l_{\rm in} = l$.

At this step one can note that the even or odd character of the index l characterizing the higher-degree term may be directly derived from the study of the current integral F_{k_1,k_2} intervening inside the angular subfactor of each term of the characteristic polynomial:

$$F_{k_1,k_2} = \int d\mathbf{S}_{k_1,k_2} Y_{l_1,m_1}(\mathbf{S}_{k_1,k_2}) Y_{l_2,m_2}(\mathbf{S}_{k_1,k_2}) \times Y_{l_3,m_3}(\mathbf{S}_{k_1,k_2}), \tag{A1}$$

with, for instance, $l_1 = l'_{k_1+1,k_2}$, $l_2 = l_{k_1-1,k_2}$, or l_{k_1,k_2} and $l_3 = l'_{k_1,k_2}$. For the four lattice corners, F_{k_1,k_2} reduces to two spherical harmonics so that there are only four selection rules between the coefficients $l_{i,j}$ and $l'_{i,j}$ on the one hand and the coefficients $m_{i,j}$ and $m'_{i,j}$ on the other hand. But more generally, for the in-sites of the lattice, F_{k_1,k_2} is given by Eq. (A1) and can be expressed by means of Clebsch-Gordan (CG) coefficients, i.e., $[(2l_1+1)(2l_2+1)/4\pi(2l_3+1)]^{1/2} C^{l_3\,0}_{l_1\,0\,l_2\,0} C^{l_3\,m_3}_{l_1\,m_1\,l_2\,m_2}$. Under these conditions the first CG coefficient does not vanish if $l_1+l_2+l_3$ is even (or null) and the second one if

$$m_1 + m_2 = m_3. \tag{A2}$$

Therefore, for the in-sites, there are no more selection rules over the coefficients $l_{i,j}, l'_{i,j}$ (which only obey triangular inequalities) and the $m_{i,j}$'s and the $m'_{i,j}$'s, respectively. Note that all these results can be also derived by studying the parity of the associated Legendre polynomials which can be written from the corresponding spherical harmonics [cf. Eq. (A1)].

Thus, if $l_1 = l_2 = l_3 = l$, that implies that l is even (or null) for the higher-degree term. In addition, there exist $(2N+1)^2-2$ equations such as Eq. (A2) for $3N(2N+1)-2$ unknowns $m_{i,j}$, and $m'_{i,j}$ so that there are $[3N(2N+1)-2]-[(2N+1)^2-2]$, i.e., $(2N+1)(N-1)$ independent over $\mathbb{Z}$ solutions $(\ldots, m_{i,j}, m'_{i,j}, \ldots)$. In other words, in the most general case, if $l_{i,j} \neq 0$ and $l'_{i,j} \neq 0$, the $m_{i,j}$'s and $m'_{i,j}$'s are not necessarily equal to zero (which is the trivial solution) and, for a finite lattice (i.e., for a finite N), there is no analytical expression for all the terms of the characteristic polynomial showing nonvanishing l values. Finally, $Z_N(0)$ does not show a unique closed-form expression, except in the thermodynamic limit.

Consequently, in this limit (i.e., for an infinite lattice), the zero-field partition function may be written under the general form

$$Z_N(0)=(4\pi)^{3N(2N+1)}\left[\sum_{l=0}^{+\infty}(\Lambda_l^{\mathrm{ed}})^{4N}(\Lambda_l^{\mathrm{in}})^{N(2N-3)}\sum_{\{m=-l\}}^{\{m=+l\}}+\sum_{\{l_{\mathrm{ed}}>0\}}\Lambda_{\{l_{\mathrm{ed}}\}}^{\mathrm{ed}}\sum_{\substack{l_{\mathrm{in}}=0\\ l_{\mathrm{in}}\notin\{l_{\mathrm{ed}}\}}}^{+\infty}(\Lambda_{l_{\mathrm{in}}}^{\mathrm{in}})^{N(2N-3)}\sum_{\{m_{\mathrm{ed}}=-l_{\mathrm{ed}}\}}^{\{m_{\mathrm{ed}}=+l_{\mathrm{ed}}\}}\sum_{\{m_{\mathrm{in}}=-l_{\mathrm{in}}\}}^{\{m_{\mathrm{in}}=+l_{\mathrm{in}}\}}+\cdots\right]$$
$$\times\prod_{k_1=-N}^{+N}\prod_{k_2=-N}^{+N}F_{k_1k_2}\quad\text{as}\quad N\to+\infty, \tag{A3}$$

where the extra factors of argument βJ characterized by a superscript independent of N (tending to infinity) have been dropped. In the leader term, the symbolical notation $\{m\}$ refers to the $3N(2N+1)-2$ summations over the $m_{i,j}$'s and $m'_{i,j}$'s (thus recalling that they belong to the set labeled $\{m\}$). Similarly, for the second term, the symbol $\{l_{\mathrm{ed}}\}$ or $\{m_{\mathrm{ed}}\}$ concerns the $4(3N-1)$ summations over coefficients l_{ed} or m_{ed} (respectively, l'_{ed} or m'_{ed}) characterizing the edge bonds (and belonging to the set labeled $\{l_{\mathrm{ed}}\}$ or $\{m_{\mathrm{ed}}\}$), whereas the symbol $\{m_{\mathrm{in}}\}$ refers to the $3N(2N-3)+2$ summations over the coefficients $m_{i,j}$ and $m'_{i,j}$ characterizing the inside bonds (and elements of the set labeled $\{m_{\mathrm{in}}\}$). The ellipsis (representing the terms of lower degree) is made of a product of $3N(2N-3)-2$ functions $\lambda_l(-\beta j)$, $j=J_0$, or J, with different coefficients l. If the l's are equal for a given argument βj, the highest value of the corresponding superscript is at most equal to $N(2N+1)$ if $j=J_0$ [respectively, $2N(2N+1)-2$ if $j=J$]. If that case occurs, the other contribution of argument βJ (respectively, βJ_0) giving the higher-degree term of these second-rank factors is characterized by a superscript lower than $2N(2N+1)-2$ [respectively, $N(2N+1)$], the other factors of similar argument being characterized by a mixture of coefficients l.

*Author to whom correspondence should be addressed.
Fax: +(33) 556-84-69-70. Electronic address:
rouch@decalpha.cpmoh.u-bordeaux.fr

[1] L. J. De Jongh and A. R. Miedema, Adv. Phys. **23**, 1 (1974); *Magnetic Properties of Layered Transition Metal Compounds*, edited by L. J. De Jongh, Physics and Chemistry of Materials with Low-Dimensional Structures Vol. 9A (Kluwer Academic, Dordrecht, 1989) and references therein.
[2] J. G. Bednorz and K. A. Müller, Z. Phys. B **64**, 189 (1986).
[3] F. Legrand and R. Plumier, Phys. Status Solidi **2**, 317 (1962); J. Phys. Radium **23**, 474 (1962); K. G. Srivastava, Phys. Lett. **4**, 55 (1963); M. E. Lines, Phys. Rev. **156**, 543 (1967); **164**, 736 (1967).
[4] Y. Ishikawa and S. Akimoto, J. Phys. Soc. Jpn. **13**, 1298 (1958); A. Sawaoka, S. Miyahara, S. Akimoto, and H. Fujisawa, *ibid.* **21**, 185 (1966).
[5] G. Shirane, S. I. Pickart, and Y. Ishikawa, J. Phys. Soc. Jpn. **14**, 1352 (1959).
[6] J. Akimitsu, Y. Ishikawa, and Y. Endoh, Solid State Commun. **8**, 87 (1970).
[7] J. J. Stickler, S. Kern, A. Wold, and G. S. Heller, Phys. Rev. **164**, 765 (1967).
[8] H. Yamauchi, H. Hiroyoshi, M. Yamada, H. Watanabe, and H. Takei, J. Magn. Magn. Mater. **31-34**, 1071 (1983).
[9] G. De Munno, M. Julve, F. Nicolò, F. Lloret, J. Faus, R. Ruiz, and E. Sinn, Angew. Chem. Int. Ed. Engl. **32**, 613 (1993).
[10] G. De Munno, R. Ruiz, F. Lloret, J. Faus, R. Sessoli, and M. Julve, Inorg. Chem. **34**, 408 (1995).
[11] M. Julve, M. Verdaguer, O. Kahn, A. Gleizes, and M. Philoche-Levisalles, Inorg. Chem. **23**, 3808 (1984); M. Julve, M. Verdaguer, G. De Munno, J. A. Real, and G. Bruno, *ibid.* **32**, 795 (1993).
[12] P. Román, C. Guzmán-Miralles, A. Luque, J. I. Beita, J. Cano, F. Lloret, M. Julve, and S. Alvarez, Inorg. Chem. **35**, 3741 (1996); G. De Munno, M. Julve, F. Lloret, and A. Derory, J. Chem. Soc. Dalton Trans. **1993**, 1179 (1993).
[13] J. T. Wrobleski and D. Brown, Inorg. Chem. **18**, 498 (1979); E. Andrés, G. De Munno, M. Julve, J. A. Real, and F. Lloret, J. Chem. Soc. Dalton Trans. **1993**, 2169 (1993).
[14] (a) D. Deguenon, G. Bernardelli, J. P. Tuchagues, and P. Castan, Inorg. Chem. **29**, 3031 (1990); (b) J. Glerup, P. A. Goodson, D. J. Hodgson, and K. Michelsen, *ibid.* **34**, 6255 (1995); (c) G. De Munno, T. Poerio, M. Julve, F. Lloret, G. Viau, and A. Caneschi, J. Chem. Soc. Dalton Trans. **1997**, 601 (1997); (d) G. De Munno, G. Viau, M. Julve, F. Lloret, and J. Faus, Inorg. Chim. Acta **250**, 81 (1997).
[15] J. Curély, Europhys. Lett. **32**, 529 (1995) and references therein.
[16] (a) J. Curély, Physica B **245**, 263 (1998), and references therein; (b) Physica B (to be published); (c) J. Curély and J. Rouch, Physica B (to be published).
[17] M. E. Fisher, Am. J. Phys. **32**, 343 (1964).
[18] S. Chakravarty, B. I. Halperin, and D. R. Nelson, Phys. Rev. B **39**, 2344 (1989) and references therein.
[19] N. Elstner, A. Sokol, R. R. P. Singh, M. Greven, and R. J. Birgeneau, Phys. Rev. Lett. **75**, 938 (1995) and references therein.
[20] M. E. Lines, J. Phys. Chem. Solids **31**, 101 (1970).
[21] L. J. De Jongh, in *Magnetism and Magnetic Materials*, edited by C. D. Graham and J. J. Rhyne, AIP Conf. Proc. No. **10** (AIP, New York, 1972), p. 561.